



# Utica/Point Pleasant brine isotopic compositions ( $\delta^7\text{Li}$ , $\delta^{11}\text{B}$ , $\delta^{138}\text{Ba}$ ) elucidate mechanisms of lithium enrichment in the Appalachian Basin

Bonnie McDevitt <sup>a,\*</sup>, Travis L. Tasker <sup>b</sup>, Rachel Coyte <sup>c</sup>, Madalyn S. Blondes <sup>a</sup>, Brian W. Stewart <sup>d</sup>, Rosemary C. Capo <sup>d</sup>, J. Alexandra Hakala <sup>e</sup>, Avner Vengosh <sup>f</sup>, William D. Burgos <sup>g</sup>, Nathaniel R. Warner <sup>g</sup>



<sup>a</sup> U.S. Geological Survey, Geology, Energy & Minerals Science Center, Reston, VA, United States of America

<sup>b</sup> Saint Francis University, Department of Environmental Engineering, Loretto, PA, United States of America

<sup>c</sup> New Mexico Institute of Mining and Technology, Earth and Environmental Science Department, Socorro, NM, United States of America

<sup>d</sup> University of Pittsburgh, Department of Geology and Environmental Science, Pittsburgh, PA, United States of America

<sup>e</sup> Department of Energy, National Energy Technology Laboratory (NETL), Pittsburgh, PA, United States of America

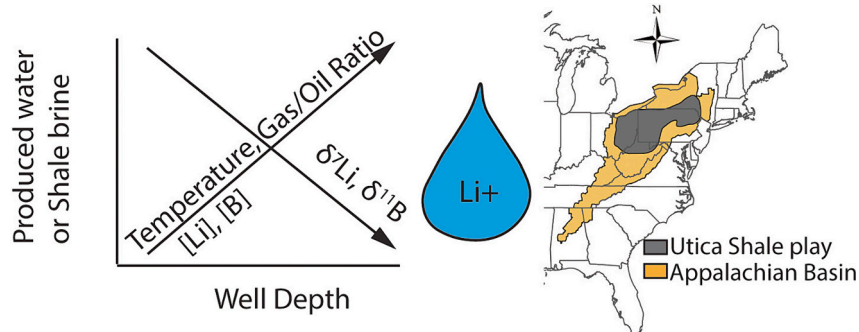
<sup>f</sup> Duke University, Nicholas School of the Environment, Durham, NC, United States of America

<sup>g</sup> The Pennsylvania State University, Department of Civil and Environmental Engineering, State College, PA, United States of America

## HIGHLIGHTS

- $\delta^7\text{Li}$ ,  $\delta^{11}\text{B}$ ,  $\delta^{138}\text{Ba}$  were determined for Utica produced water and core.
- Utica and Marcellus produced water  $\delta^7\text{Li}$ ,  $\delta^{11}\text{B}$ ,  $\delta^{138}\text{Ba}$  reflect no differences.
- Depth-dependent thermal maturity likely control [Li] in Utica produced water.
- Utica produced water [Li] is highest where the Mg/Li ratios and  $\delta^7\text{Li}$  are lowest.

## GRAPHICAL ABSTRACT



## ARTICLE INFO

Editor: Christian Herrera

**Keywords:**  
Oil and gas  
Produced water  
Commodity  
Renewable energy  
Thermal maturity

## ABSTRACT

Global Li production will require a ~500 % increase to meet 2050 projected energy storage demands. One potential source is oil and gas wastewater (i.e., produced water or brine), which naturally has high total dissolved solids (TDS) concentrations, that can also be enriched in Li (>100 mg/L). Understanding the sources and mechanisms responsible for high naturally-occurring Li concentrations can aid in efficient targeting of these brines. The isotopic composition ( $\delta^7\text{Li}$ ,  $\delta^{11}\text{B}$ ,  $\delta^{138}\text{Ba}$ ) of produced water and core samples from the Utica Shale and Point Pleasant Formation (UPP) in the Appalachian Basin, USA indicates that depth-dependent thermal maturity and water-rock interaction, including diagenetic clay mineral transformations, likely control Li concentrations. A survey of Li content in produced waters throughout the USA indicates that Appalachian Basin brines from the Marcellus Shale to the UPP have the potential for economic resource recovery.

\* Corresponding author at: U.S. Geological Survey, 12201 Sunrise Valley Dr, MS 954, Reston, VA 20192, United States of America.

E-mail address: [bmcdevitt@usgs.gov](mailto:bmcdevitt@usgs.gov) (B. McDevitt).

## 1. Introduction

The world's demand for lithium (Li) in energy storage capabilities will require a ~500 % increase from 2018 production to meet 2050 demands (Hund et al., 2020). Lithium is included on the U.S. Geological Survey's Critical Mineral List (Federal Register: U.S. Geological Survey, 2022), and deemed both a high energy demand and high security risk raw material by the U.S. Department of Energy (U.S. Department of Energy, 2023). Typically, Li is sourced from mining Li-rich pegmatite rocks, mostly in Australia, or from evaporated Li-rich brines, such as those generated in the South America Lithium Triangle (i.e., Bolivia, Argentina, Chile) (Kesler et al., 2012). As with any energy development, these Li mining activities are not without their share of potential negative environmental impacts (Kaunda, 2020). Given the increasing need for Li, alternative sources for Li extraction are being explored. Formation waters, which are deep subsurface brines, represent one such source, as they frequently contain high (>100 mg/L) concentrations of Li (Blondes et al., 2018; Darvari et al., 2024; Dugamin et al., 2021; Mackey et al., 2024; Marza et al., 2024). These formation brines are generated in large volumes (estimated as 4.1 trillion L in the United States in 2021 (Groundwater Protection Council, 2022)) when co-produced with oil and natural gas (referred to as produced water). In 2021, approximately 96 % of these produced waters in the U.S. were reinjected into permeable formations underlying the source formation via underground injection control (UIC) wells as the principle method of disposal or enhanced oil recovery processes (Groundwater Protection Council, 2022). Given that some produced waters contain economic levels of Li, produced water disposal represents both a loss of water commodity (Kondash et al., 2018; McDevitt et al., 2020b; McLaughlin et al., 2020) and a lost opportunity for extracting this raw energy storage material (Kumar et al., 2019).

The Appalachian Basin, USA, which has a long history of hydrocarbon development, experienced a shale gas boom over the past 15 years with natural gas being recovered from the Devonian organic-rich Marcellus Shale and the underlying Ordovician Utica Shale and Point Pleasant Formation, referred to herein as the UPP. Recoverable natural gas estimates are 2.4 trillion cubic meters from the Marcellus Shale and 1.1 trillion cubic meters from the UPP (the first and fourth largest natural gas plays in the U.S., respectively) (Hickman et al., 2015; Kirschbaum et al., 2012). Numerous studies have characterized the large volume of produced water (millions of L per well) generated during oil and gas production (Kondash et al., 2017; Scanlon et al., 2020b, 2020a), the chemical composition and geologic origin of the produced water (Akob et al., 2015; Blondes et al., 2020; Capo et al., 2014; Dresel and Rose, 2010; Engle and Rowan, 2014; Harkness et al., 2015; Macpherson, 2015; Macpherson et al., 2014; Matecha et al., 2022; McDevitt et al., 2022; Osborn et al., 2012; Phan et al., 2016, 2015; Rowan et al., 2011; Rowan et al., 2015; Stewart et al., 2015; Welch et al., 2021, 2022), geochemical fingerprinting techniques to resolve potential contamination events (Chapman et al., 2012; Tasker et al., 2020; Tieman et al., 2020; Warner et al., 2014), and the environmental impacts of both spills and managing and disposing of the wastewater (Akob et al., 2016; Burgos et al., 2017; Cozzarelli et al., 2021; Drollette et al., 2015; Farnan et al., 2023; Geeza et al., 2018; Kassotis et al., 2016; Lauer et al., 2018; McDevitt et al., 2020a, 2021; Mumford et al., 2020; Patnode et al., 2015; Paukert Vankeuren et al., 2017; Piotrowski et al., 2020; Stallworth et al., 2021; Tasker et al., 2018; Van Sice et al., 2018; Wilson and Vanbriesen, 2012).

Appalachian Basin produced waters contain elevated salinity, often ten times higher than seawater, and high radium activity (highest reported combined  $^{226}\text{Ra} + ^{228}\text{Ra}$  is 668 Bq/L in Marcellus Shale produced water) (Rowan et al., 2011; Warner et al., 2022). Elevated Li concentrations (up to 634 mg/L) have been reported in Marcellus Shale produced water (Phan et al., 2016). Previous studies have demonstrated the use of isotope tracers ( $^{87}\text{Sr}/^{86}\text{Sr}$ ,  $^{7}\text{Li}/^{6}\text{Li}$ ,  $^{11}\text{B}/^{10}\text{B}$ ,  $^{138}\text{Ba}/^{134}\text{Ba}$ ) to better understand the evolution of Appalachian Basin brines as well as to

fingerprint (i.e., determine the origin of) and quantify contributions to overlying, less saline groundwater (Chapman et al., 2012; Kolesar Kohl et al., 2014; Macpherson et al., 2014; Phan et al., 2016; Tieman et al., 2020; Warner et al., 2014). To date, there are no Li, B, or Ba isotope data available for UPP produced water or rock core which support an expansion of our mechanistic understanding of Li enrichment and basinal heterogeneity in produced water.

Recent studies have reported high Li concentration and resource estimate commonalities observed for conventional reservoirs that include water-rock associations yielding similarly high concentrations of K, Ca, and B, proximity to major faults, and production of brines from high porosity carbonate formations due to higher fluid yields (Darvari et al., 2024; Marza et al., 2024). Continuous (or unconventional) reservoirs are typically developed using hydraulic fracturing that targets the hydrocarbon (and Li) source rocks (often shales). These reservoirs are generally characterized by low permeability and high thermal maturity, which have been shown to generate B, Li, Sr, and Ba isotope compositions that are distinct from nearby conventional reservoirs (Macpherson et al., 2014; Phan et al., 2016; Warner et al., 2014). An assessment of the origin of Li and enrichment mechanisms in the UPP has not yet been conducted but is warranted given the elevated concentrations (>80 mg/L) previously reported (Blondes et al., 2020; Tasker et al., 2020). Previous studies have demonstrated elevated levels of Li and B in produced water which were attributed to water-rock interactions associated with thermal maturation of the hydrocarbons and host geological formations (i.e., clay mineral diagenesis) (Williams et al., 2001; Williams and Hervig, 2005). Based on these studies, we hypothesize that produced water generated during unconventional oil and natural gas (shale gas) extraction from continuous reservoirs would be subject to more extensive brine-rock interactions relative to conventional produced water. Clay minerals and shales are the major source of Li and B in the earth's crust (Macpherson, 2015; Parker, 1967; Spivack et al., 1987) and preferentially incorporate the lighter  $^{6}\text{Li}$  and  $^{10}\text{B}$  isotopes from coexisting aqueous solutions which generates useful Li source and enrichment tracing tools (Millot et al., 2010b; Tomascak, 2004; Vigier et al., 2008). Similarly, barite ( $\text{BaSO}_4$ ) precipitation, often associated with black shales, preferentially incorporates isotopically lighter dissolved Ba which leads to the utility of Ba isotopes to indicate additional water-rock interactions associated with produced water (Von Allmen et al., 2010; Horner et al., 2015; Hsieh and Henderson, 2017; Wang et al., 2021). Identifying a distinct isotopic composition ( $^{7}\text{Li}/^{6}\text{Li}$ ,  $^{11}\text{B}/^{10}\text{B}$ ,  $^{138}\text{Ba}/^{134}\text{Ba}$ ) of produced water from unconventional shale plays such as the UPP that are associated with elevated Li concentrations could be useful to evaluate the potential of Li extraction from produced water across the U.S., in addition to surveys that are focused solely on elemental concentrations in produced water.

This study (1) presents new Li, B, and Ba isotope data in produced water to elucidate processes that affect fluid composition and geochemical differences between the UPP, Marcellus Shale, and other Appalachian Basin units, and (2) evaluates the geochemistry and Li isotope systematics in UPP core samples to better understand fluid-rock interactions that result in elevated Li concentrations. We also (3) apply observations linking isotopic compositions to elemental ratios presented herein for the UPP to evaluate Li abundance in produced waters throughout the U.S. and identify important knowledge gaps guiding potential Li resource exploration.

## 2. Materials and methods

### 2.1. Geological background

The Utica Shale is an Ordovician calcareous black shale containing thin K-bentonite clay beds weathered from volcanic ash (Delano et al., 1990). The extent of the Utica Shale play includes present-day U.S. states New York, Ohio, Pennsylvania, and West Virginia (Hickman et al., 2015; U.S. Energy Information Administration, 2017) (Fig. 1). The Utica Shale

overlies the organic-rich calcareous shale and interbedded limestones of the Point Pleasant Formation and, together, they are referred to herein as the UPP (Fig. S1). The UPP exhibits variable total organic carbon (1–5 %), carbonate (20–60 %) and clay (30–60 %) content (Hickman et al., 2015). The UPP overlies the Trenton Limestone, Black River Group, and dolomitic Beekmantown Group (Fig. S1). Between the unconventional Middle Devonian Marcellus Shale and UPP are the conventionally produced Devonian Oriskany, and Silurian Clinton and Medina sandstone hydrocarbon reservoirs. The Queenston Shale, Reedsville Shale and the informal Cincinnati group act as a geologic seal for the Ordovician and Cambrian hydrocarbon reservoirs though some evidence may suggest sufficient porosity to have allowed oil and gas to have escaped from the UPP into these conventional reservoirs (Ryder et al., 1998).

The UPP, like the greater Appalachian Basin, USA, represents an asymmetric depression in cross-section in association with the Rome Trough which represents an approximately 72–80 km wide rift system from the Middle Cambrian that drops basement to >7900 m below mean sea level (Ryder et al., 2009). The UPP ranges in depth from 2300 m in northwest Pennsylvania to 4000 m in West Virginia and southwestern Pennsylvania, with a rapid uplift along the Appalachian Mountain structural front as exposed outcrop (Hickman et al., 2015). UPP thickness ranges from 60 to 150 m, thinning westward from southwestern Pennsylvania to eastern Ohio.

## 2.2. Produced water samples

Produced water samples were collected in two separate field campaigns. Produced water was collected from both conventional produced water township storage tanks intended for road spreading ( $n = 10$ ) by Tasker et al. (2018) and from unconventional UPP oil and gas wells ( $n = 14$ ) by Tasker et al. (2020). Major and trace element data,  $^{87}\text{Sr}/^{86}\text{Sr}$ , and

$^{226}\text{Ra}/^{228}\text{Ra}$  were originally characterized and published by Tasker et al. (2018) and Tasker et al. (2020) (methods for those results can be located within). Briefly, in those studies, major cations and trace metals were analyzed by Inductively Coupled Plasma Optical Emission Spectroscopy (ICP-OES) and Inductively Coupled Plasma Mass Spectrometry (ICP-MS) and major anions by Ion Chromatography (IC). Matrix and mass interferences were monitored using internal spikes (Sc, In, Re, Y), check standards (SRM6140a, U.S. Geological Survey (USGS) standard reference samples USGS M-220, and USGS T-227) that produced concentrations with <5 % difference between measured and known concentrations, and matrix matched high salinity standards. The cationic-anionic charge balance was better than 10 %. This study relied on those previously published data but also performed new analyses on those previously collected produced water samples that were filtered (0.45  $\mu\text{m}$  cellulose acetate filters), acidified with nitric acid, and stored at 4 °C. A brief review of the methods to collect those produced water samples are presented here, with remaining methods focusing on the new analyses performed (e.g., Li concentrations by ICP-MS for Li isotope chromatography column yield checks and Li, B, and Ba isotopic compositions) as well as describing new UPP core samples.

Unconventional UPP produced water samples presented in this study ( $n = 14$ ) were collected from separators located at wellheads in Ohio, Pennsylvania, and West Virginia, USA (Fig. 1, Table S1) (McDevitt et al., 2024). Wellhead access, well depth, and production information were provided by industry partners and based on well production reports. To our knowledge, all wells were cased down to at least the production depths reported here. All wells selected for sampling had been in production for >120 days to ensure collection of produced water with minimal influence of externally introduced components (such as drilling or completion fluid) and to alleviate concerns about fluid mixtures (Rowan et al., 2015). True vertical depths (TVD) for the unconventional UPP wells ranged from 2285 to 4116 m.

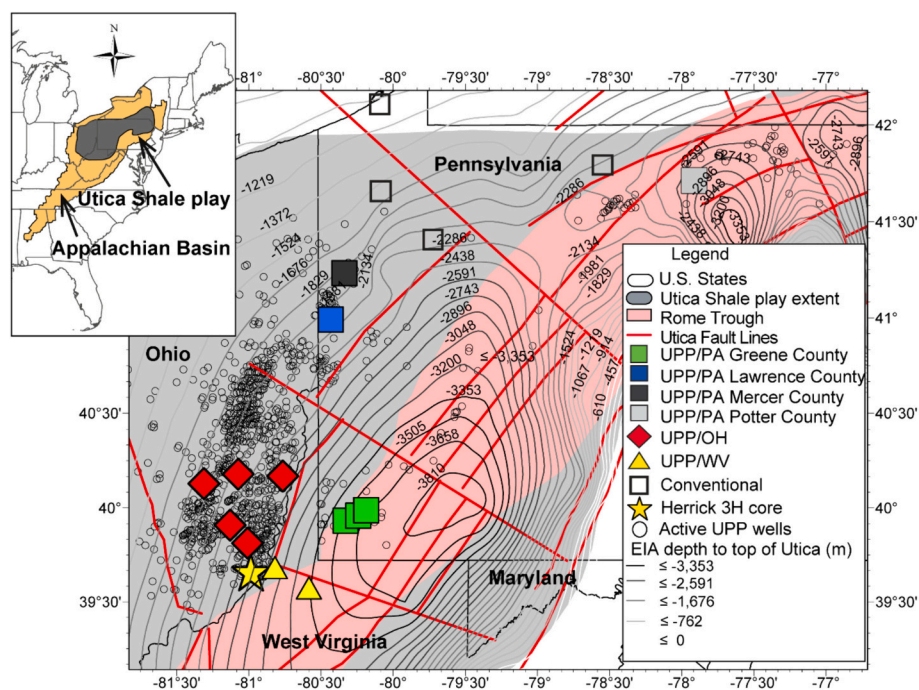


**Fig. 1.** Map of the Utica Shale and Point Pleasant Formation (UPP) study area within the larger Appalachian Basin. The inset U.S. map indicates the larger Appalachian Basin extent (yellow) and Utica Shale play extent (gray). UPP samples were collected from Pennsylvania (PA), Ohio (OH), and West Virginia (WV) ( $n = 14$ ) (Tasker et al., 2020). For the UPP samples collected in PA (UPP/PA), county names are also designated as varying symbol color fill. Actively producing UPP wells are plotted as unfilled circles for visual well density (from Pennsylvania Department of Environmental Protection ([pasda.psu.edu](http://pasda.psu.edu)) and Ohio Department of Natural Resources ([gis.ohiodnr.gov](http://gis.ohiodnr.gov))). The National Energy Technology Laboratory's UPP Herrick 3H well location from which three core samples were derived is designated by a yellow star. Depth profiles (contours) for the UPP measured as depth to the top of the UPP from sea level and pre-UPP fault lines (red) from U.S. Energy Information Administration (EIA) (U.S. Energy Information Administration, 2017) are included for reference along with the Rome Trough Appalachian Basin geologic feature. County centroids ( $n = 4$ ) for conventional samples ( $n = 10$ ) are represented by unfilled black squares as the geographic coordinates of the county center.

Unconventional UPP well gas-oil-ratios (GORs) were calculated using data from S&P Global Commodity Insights (S&P Global Commodity Insights, 2023); the cumulative gas produced in each well was divided by the cumulative oil produced and presented in units of cubic foot of gas per barrel of oil (CFB). GORs were used to systematically assign a hydrocarbon type classification according to the Society of Petroleum Engineers range for gas condensate (3500–30,000 CFB), wet gas (30,000+ CFB), and dry gas (i.e., no oil produced). S&P Global Commodity Insights (S&P Global Commodity Insights, 2023) did not contain information for every unconventional UPP well sampled in this study; therefore, GOR data for those wells (4 of the 14) were omitted. Additionally, S&P Global Commodity Insights (S&P Global Commodity Insights, 2023) was utilized to mine available UPP well ( $n = 10$ ) cumulative water production for calculation of estimated Li production per well lifetime.

Conventional produced water samples ( $n = 10$ ) were collected from Pennsylvania township brine storage tanks intended for road spreading as dust suppression and de-icing. Locations of storage tanks are provided at the county level to maintain township anonymity (Table S1). Conventional produced water well samples represent the informal Bradford group, as well as the Oriskany, Beekmantown, and Medina Groups. Geologic unit identification for produced water in each storage tank was provided by township road supervisors as sampling did not occur at wellheads. Four samples (PA06, PA07, PA09, PA12) represent a produced water mixture from two distinct geologic units (Table S1).

### 2.3. Utica Herrick 3H core samples

Three Utica core samples were donated by National Energy Technology Laboratory (NETL) from the Herrick 3H vertical well located in Monroe County, Ohio, USA (Brown et al., 2018). The entire Herrick 3H core spans vertical Utica Shale depths ranging from 3219 m to 3311 m. The Herrick 3H core is described as fine-grained shale with layers of organic-rich and fossiliferous calcareous shale and silty mudstone (Brown et al., 2018). Core samples were selected for this study at three distinct vertical depths (3230.8 m, 3261.4 m, and 3310.7 m) and were chosen at approximately even depth intervals spanning the length of the core, representing one sample from each of three sub-cores stored at NETL (Brown et al., 2018). NETL personnel split the core samples according to their specific core preservation strategy and shipped samples to The Pennsylvania State University for analysis. Core sample 3230.8 m was denoted as shale-rich with some nodules and rounded clasts with fewer calcareous layers and fossils. Core sample 3261.4 m represented a core section with organic-rich layers alternating with calcareous, fossil-rich sections containing marine shells. The deepest sample, 3310.7 m represented calcareous shale and fossiliferous silty mudstone with more apparent vertical fractures. Upon receipt, the core sample was ground with mortar and pestle to homogeneity and ashed to prevent high organic content interference with the Li isotope chromatography, as determined from previous shale analyses. Ashing methods and loss on ignition calculation are included in more detail in the Supporting Information. Approximately 0.1 g of ashed core was subsequently digested in Teflon vessels utilizing trace grade nitric acid, hydrofluoric acid, perchloric acid, hydrochloric acid, and hydrogen peroxide. See Supplemental Information for a detailed digestion procedure. Once digested, ashed core samples were analyzed for major cations and select trace elements (Li, B, Ba, Ca, Fe, K, Mg, Na, Sr) via ICP-OES in the Laboratory for Isotopes and Metals in the Environment (LIME) at The Pennsylvania State University (Table S2). A standard rock, USGS SGR-1 (U.S. Geological Survey, 2022), was processed and analyzed simultaneously with Herrick 3H core samples for comparison to literature and to identify any impacts of the ashing and digestion procedure on bulk chemistry. From the simultaneous analysis of USGS SGR-1, most major and trace cation concentrations analyzed and reported were either within or elevated compared to literature reported bulk rock chemistry (Jochum et al., 2005) except for bulk B concentrations, likely due to the high

temperature ashing procedure employed that induced a loss of B. Thus, we do not provide interpretations related to B concentrations in the UPP core. Previous studies of USGS SGR-1 did not include this additional rock ashing procedure (Phan et al., 2016; Pogge von Strandmann et al., 2017).

### 2.4. Isotope analysis

Delta values for all isotopic systems were calculated according to the following equation:

$$\delta(\text{‰}) = \left( \frac{\text{Ratio}_{\text{sample}}}{\text{Ratio}_{\text{standard}}} - 1 \right) \times 1000 \quad (1)$$

#### 2.4.1. Lithium

Lithium isotopes ( $^7\text{Li}/^6\text{Li}$ ) in produced water samples and digested core samples were measured in the LIME Laboratory at The Pennsylvania State University. 150 ng of Li was processed and chemically separated in each sample utilizing cationic resin (2 mL of AG50W-X12 (200–400 mesh) resin in a 9 cm Bio-Rad column with a hydrophilic frit) and trace grade 0.2 N HCl. Targeted sample volumes were evaporated in Teflon vials on a hotplate at 70 °C, re-dissolved in 0.2 mL of trace grade 0.2 N HCl, and loaded into Bio-Rad columns. Lithium yield checks were conducted by measuring permeate on a Thermo XSeries II ICP-MS and indicated >98 % mass recovery of Li through Bio-Rad chromatography.  $^7\text{Li}/^6\text{Li}$  in standards (Alfa Asar and SRM 3129a) and samples were analyzed on a Neptune multi-collector ICP-MS (MC-ICP-MS) bracketed by two blanks (blank correction) and two IRMM-16 standards (NIST replacement for LSVEC) to calculate  $\delta^7\text{Li}$  as a per mil deviation from IRMM-16 according to Eq. (1). Average SRM 3129a  $\delta^7\text{Li}$  was  $6.44\text{‰} \pm 0.38\text{‰}$  (2 $\sigma$ ) ( $n = 15$ ). Average Alfa Asar  $\delta^7\text{Li}$  was  $80.79\text{‰} \pm 0.36\text{‰}$  (2 $\sigma$ ) ( $n = 15$ ). A method standard check was conducted utilizing IAPSO seawater which yielded a  $\delta^7\text{Li}$  value of  $31.35\text{‰} \pm 0.34\text{‰}$  (2 $\sigma$ ) ( $n = 2$ ), which fell within the reported literature range (Andrews et al., 2020; Jochum et al., 2005; McDevitt et al., 2020b; Pogge von Strandmann et al., 2008).

#### 2.4.2. Boron

Boron isotopes ( $^{11}\text{B}/^{10}\text{B}$ ) in produced water samples were measured at Duke University using a Triton (ThermoFisher) thermal ionization mass spectrometer (TIMS). Produced water samples were diluted to around 2 ppm B and 1 mL aliquots were pre-treated with 50  $\mu\text{L}$  of 10 % trace grade hydrogen peroxide. After one week of pre-oxidation in a vertical laminar flow clean hood equipped with boron-free PTFE HEPA filtration, 3–10 ng of B per sample was loaded onto single Re filaments with boron free seawater and measured in negative mode as  $\text{BO}_2^-$  ions.  $^{11}\text{B}/^{10}\text{B}$  values were then normalized to NIST SRM 951 standard and reported as  $\delta^{11}\text{B}$  using Eq. (1). NIST SRM 951 average  $^{11}\text{B}/^{10}\text{B}$  value for the six months before and six months after the analysis was  $4.0053 \pm 0.0022$  ( $n = 33$ ).

#### 2.4.3. Barium

Produced water samples for Ba isotope analysis were prepared under Class 100 conditions (ISO 14644-1 Equivalent ISO 5) in the isotope geochemistry clean lab at the University of Pittsburgh. A  $^{137}\text{Ba}$ – $^{135}\text{Ba}$  double spike was added to each sample aliquot prior to processing in order to correct for isotope fractionation caused by chromatographic separation of Ba from the sample matrix using the method detailed in Matecha et al. (2021). Barium isotope composition was analyzed on a Thermo Neptune Plus MC-ICP-MS at the University of Pittsburgh. Eight Faraday collectors were used to simultaneously measure abundances of  $^{134}\text{Ba}$ ,  $^{135}\text{Ba}$ ,  $^{136}\text{Ba}$ ,  $^{137}\text{Ba}$ , and  $^{138}\text{Ba}$  and three interfering elements. Isobaric interferences from  $^{134}\text{Xe}$ ,  $^{136}\text{Xe}$ ,  $^{136}\text{Ce}$ ,  $^{138}\text{Ce}$ , and  $^{138}\text{La}$  were corrected using the masses of non-overlapping isotopes  $^{131}\text{Xe}$ ,  $^{139}\text{La}$ , and  $^{140}\text{Ce}$ . Barium isotope ratios reported as  $\delta^{138}\text{Ba}$  are normalized to NIST 3104a using Eq. (1). Further details of the measurement method are

reported in the Supplementary Information of [Tieman et al. \(2020\)](#).

### 2.5. Previously published produced water data mining

Previously published Appalachian Basin geochemical data were compiled from literature ([Blondes et al., 2020](#); [Capo et al., 2014](#); [Chapman et al., 2012](#); [Macpherson et al., 2014](#); [Phan et al., 2016](#); [Tasker et al., 2020](#); [Tieman et al., 2020](#); [Warner et al., 2014](#)) for comparison to the isotopic measurements in this study. Only studies that expressly indicated produced water was sampled >90 days into well production were considered so that both geochemical steady state could be cautiously assumed for these samples and there would be enough data for comparison ([Chapman et al., 2012](#); [Engle and Rowan, 2014](#); [Phan et al., 2016](#); [Warner et al., 2014](#)). While this requirement drastically reduces the number of data points for comparison, it is a necessary culling step to avoid misinterpretation of potential flowback contribution and instead characterize the native formation brines.

## 3. Results and discussion

### 3.1. UPP and Appalachian Basin produced water Li, B, and Ba geochemistry

Lithium concentrations range from 33.7 to 85.9 mg/L in the UPP produced water ( $n = 14$ ) measured in this study while B concentrations range from 4.8 to 30.3 mg/L (Table S1). Li and B concentrations in UPP produced water are positively and significantly correlated (Fig. S2,  $R^2 = 0.72$ ,  $p = 1.7E-4$ ), with the highest Li and B concentrations co-occurring in Greene County, Pennsylvania at depths up to 4116 m. UPP Ba concentrations for samples in this study range from 57 to 2611 mg/L. UPP  $\delta^{7\text{Li}}$  ( $8.34 \pm 0.90 \text{ ‰}$  –  $13.78 \pm 0.29 \text{ ‰}$ ) and  $\delta^{11\text{B}}$  (26–35 ‰) values are relatively low compared to present-day seawater (31 ‰ and 39 ‰, respectively) ([Foster et al., 2010](#)). However, UPP produced water  $\delta^{7\text{Li}}$  values fall within the expected ranges published for Ordovician seawater ([Kalderon-Asael et al., 2021](#); [Lin et al., 2024](#)).  $\delta^{138\text{Ba}}$  values for UPP

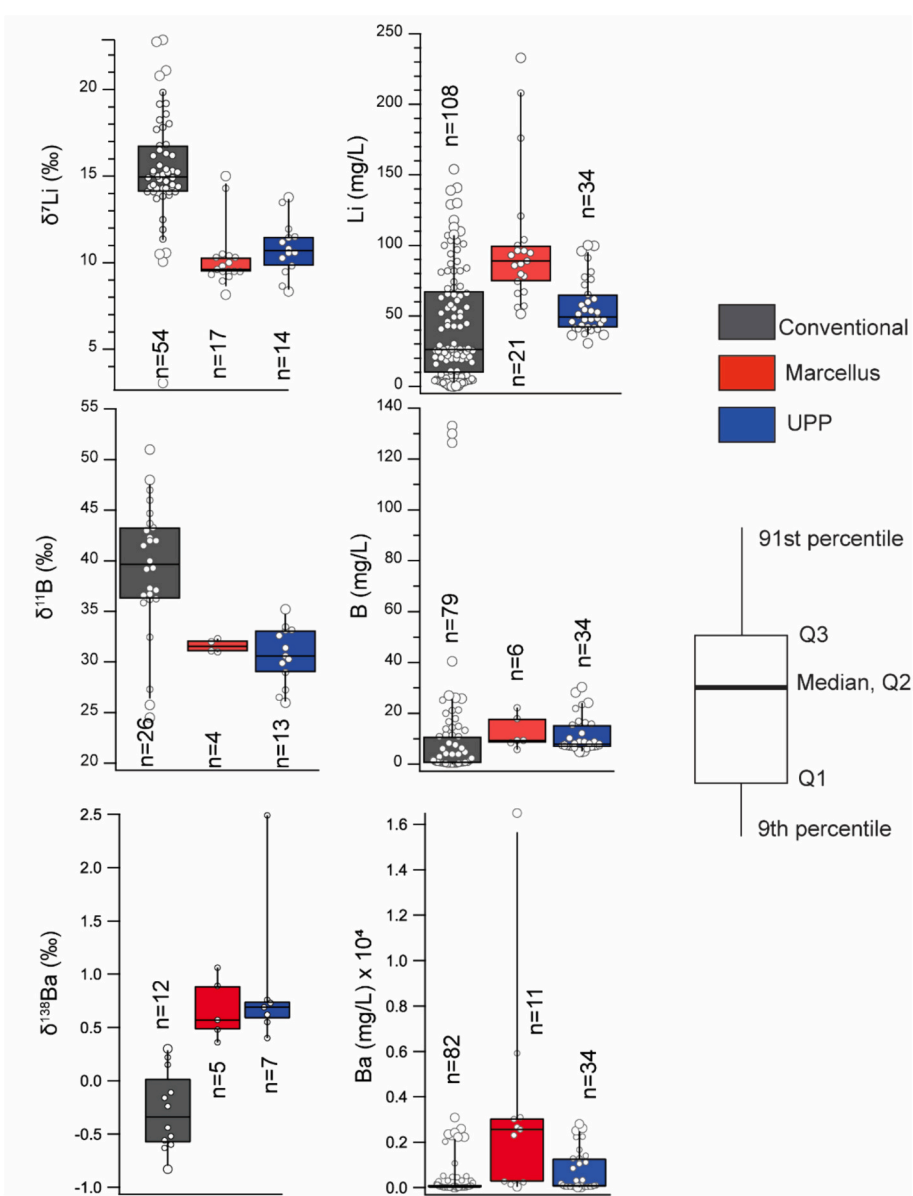


**Fig. 2.** Box and whisker plots of Li, B, and Ba concentrations and respective isotopic compositions in produced water samples from conventional, Marcellus Shale and Utica Shale and Point Pleasant Formation (UPP) wells in the Appalachian Basin, USA. Data for this study was supplemented from other studies ([Blondes et al., 2020](#); [Capo et al., 2014](#); [Chapman et al., 2012](#); [Macpherson et al., 2014](#); [Phan et al., 2016](#); [Tasker et al., 2020](#); [Tieman et al., 2020](#); [Warner et al., 2014](#)) for produced water collected from wells in production for >90 days. Larger circles for individual data points indicate outliers according to the percentiles indicated in the legend.

produced water range from  $0.40 \pm 0.04 \text{ ‰}$  in southeastern Ohio (UPP1) to  $2.49 \pm 0.03 \text{ ‰}$  in northwestern Pennsylvania (UPP20) which are generally higher than global seawater ( $0.17\text{--}0.65 \text{ ‰}$ ) (Bates et al., 2017; Cao et al., 2016; Horner et al., 2015; Hsieh and Henderson, 2017). Most notably, produced water from UPP20 (collected in Potter County, PA) has the highest  $\delta^{138}\text{Ba}$  value measured to date of  $2.49 \pm 0.03 \text{ ‰}$ .

Previous studies went to great length to develop geochemical tracers between UPP, Marcellus, and conventional Upper Devonian produced water, with an emphasis on identifying unique tools for contaminant sourcing (Blondes et al., 2020; Chapman et al., 2012; Geeza et al., 2018; McDevitt et al., 2021; Rowan et al., 2011; Tasker et al., 2020; Tieman et al., 2020; Warner et al., 2013, 2014). Our data suggest that there is no significant difference between UPP and Marcellus produced water  $\delta^7\text{Li}$ ,  $\delta^{11}\text{B}$ , or  $\delta^{138}\text{Ba}$  ( $p > 0.05$ ) values (Fig. 2). There is also no significant difference between UPP and Marcellus B and Ba concentrations ( $p > 0.05$ ). However, Marcellus produced water Li concentrations are significantly higher than UPP produced water Li concentrations; the average Li concentration of Marcellus produced water is  $101 \text{ mg/L}$  ( $n = 21$ ) compared to an average value of  $56 \text{ mg/L}$  ( $n = 34$ ) in the UPP ( $p < 0.001$ ).  $\delta^7\text{Li}$  and  $\delta^{11}\text{B}$  values are significantly ( $p < 0.001$ ) higher in conventional produced water compared to unconventional Marcellus and UPP produced water, while the  $\delta^{138}\text{Ba}$  value of conventional produced water is significantly lower than that of unconventional produced water ( $p < 0.005$ ).

### 3.2. Li enrichment in produced water at increased UPP depth, temperature, and hydrocarbon thermal maturity

Our data suggest that produced water geochemical heterogeneity within the UPP likely results from a depth- and temperature-dependent thermal maturity gradient, which allows for the economic production of hydrocarbons ranging from the dry gas to oil window. B concentrations are positively correlated with well depth for UPP produced water samples measured in this study (Fig. S3c,  $R^2 = 0.81$ ,  $p = 1.3\text{E-}5$ ). Li concentrations exhibit more variation across sample depth (Fig. S3a,  $R^2 = 0.36$ ,  $p = 0.02$ ); however, Li concentrations in UPP produced water increase approximately two-fold between the shallowest and deepest wells. Similarly,  $\delta^7\text{Li}$  and  $\delta^{11}\text{B}$  values exhibit inverse correlations with UPP depth ( $R^2 = 0.82$ ,  $p = 1.4\text{E-}5$  and  $R^2 = 0.46$ ,  $p = 0.01$ , respectively; Fig. 3). The decreasing  $\delta^7\text{Li}$  and  $\delta^{11}\text{B}$  values in the UPP produced water are generally associated with increasing Li and B concentrations, respectively (Fig. S3b and S3d). It is important to note that decreasing depth in the UPP directly corresponds to a southeast to northwest transect of the Appalachian Basin (Fig. 1). Previous data from this transect reflects decreasing thermal maturity of the Devonian shale; this trend is likely also similar for the underlying UPP (Bruner and Smosna, 2015; Macpherson, 2015; Rowan, 2006). The Alleghanian orogeny tectonic thrusting, on this same transect, is postulated to have driven fluids out of the deeper Appalachian Basin in the east towards the western section of the basin (Evans and Battles, 1999; Osborn et al., 2012). Previous studies have determined that produced water in the Marcellus Shale and UPP originated from relics of evaporated seawater (Blondes et al., 2020; Capo et al., 2014; Rowan et al., 2015). Yet the relative enrichment of Li and the high Li/Cl ratios in the produced water far exceed the expected Li concentrations and Li/Cl ratios from seawater evaporation alone (Vengosh et al., 1995), while normalizing to the TDS of the produced waters.

Consequently, evaporation of ancient seawater alone cannot account for the elevated Li concentrations in the produced water without considering water-rock interactions such as Li-bearing mineral diagenesis (Marza et al., 2024). Such diagenesis reactions include clay minerals as a primary source and organic matter and sulfide degradation as a possible secondary process (Dugamin et al., 2023; Macpherson et al., 2014; Phan et al., 2016; Rowan et al., 2015).  $\delta^7\text{Li}$  is a useful isotopic tool for tracking clay mineral weathering (Millot et al., 2010b; Tomascak, 2004; Vigier et al., 2008). Clay minerals and shales are the major source

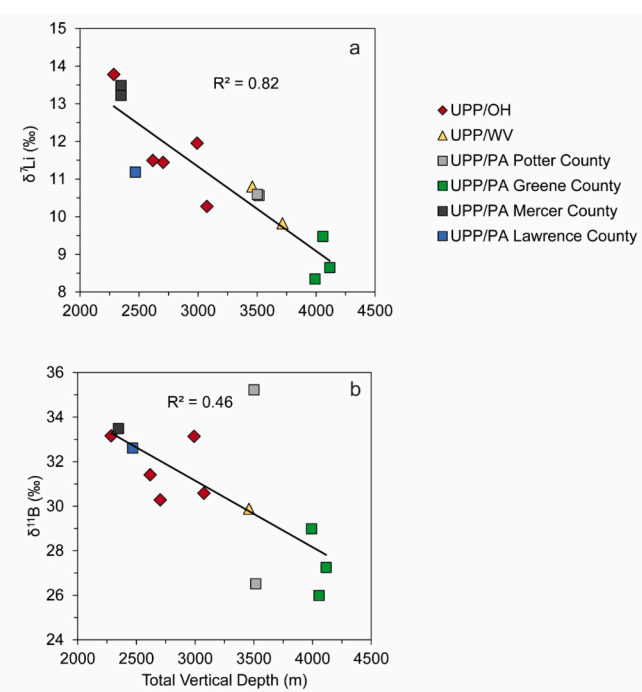


Fig. 3. a)  $\delta^7\text{Li}$  and b)  $\delta^{11}\text{B}$  values decrease with increasing Utica Shale and Point Pleasant Formation (UPP) depth, potentially indicating increasing temperatures at depth and progressive illitization of clay minerals inducing isotopic fractionation.

of Li and B in the earth's crust (Macpherson, 2015; Parker, 1967; Spivack et al., 1987) and preferentially incorporate the lighter  $^6\text{Li}$  and  $^{10}\text{B}$  isotopes from coexisting aqueous solutions (Pistiner and Henderson, 2003; Rudnick et al., 2004). It has been postulated that the diagenetic modification of smectite to illite induces isotopic fractionation by mobilizing the light isotopes  $^6\text{Li}$  and  $^{10}\text{B}$  into the illite mineral lattice and is inversely correlated with temperature up to  $100 \text{ }^\circ\text{C}$  (Macpherson, 2015; Millot et al., 2010a; Osborn et al., 2012). Thus, the decreasing  $\delta^7\text{Li}$  and  $\delta^{11}\text{B}$  values with depth in the UPP observed in this study potentially indicate Li and B mobilization from clay minerals impacted by clay diagenesis during thermal maturation of both the hydrocarbons and the host source rocks (Perry and Hower, 1970; Williams et al., 2013).

While Ba isotopes in UPP samples do not show the same systematic variation with depth or temperature observed in the Li and B isotope values, there is a clear difference between unconventional shale gas produced water (high  $\delta^{138}\text{Ba}$  values) and conventional oil and gas produced water (low  $\delta^{138}\text{Ba}$  values; Fig. 2). One explanation for this could be precipitation of barite ( $\text{BaSO}_4$ ), a mineral often associated with black shale (Renock et al., 2016). As barite precipitates, it preferentially incorporates isotopically light Ba isotopes, leading to an aqueous fluid enriched in  $^{138}\text{Ba}$  (i.e., high  $\delta^{138}\text{Ba}$ ) (Von Allmen et al., 2010; Horner et al., 2015; Hsieh and Henderson, 2017; Wang et al., 2021). However, barite precipitation would rapidly decrease the Ba concentration in the residual fluid and thus cannot explain both the high Ba concentrations and high  $\delta^{138}\text{Ba}$  values in the unconventional shale gas produced waters (Matecha et al., 2022; Tieman et al., 2020). We hypothesize instead that Ba exchange between the formation water and exchangeable sites on clay and organic matter could explain the high  $\delta^{138}\text{Ba}$  values observed in the formation water, as this process leaves dissolved Ba concentrations largely unaffected. Previous work has shown that Ba adsorbed on mineral surfaces tends to be isotopically lighter than that in the coexisting fluid (Bridgestock et al., 2021; Gong et al., 2020). Therefore, long-term interaction of high-TDS fluids with shale at depth may result in formation waters enriched in  $^{138}\text{Ba}$ . While the Ba isotopic systematics of deep formation waters and diagenetic clay transformations are largely

unexplored, the data presented here suggest that, as with Li concentrations and isotopic compositions, fluid-rock or fluid-clay interaction plays a critical role in controlling formation water composition.

Utilizing a Mg—Li geothermometer calculation (Kharaka and Mariner, 1989), temperatures were positively associated with increasing UPP well depth (Fig. S4,  $R^2 = 0.87, p = 1.3E-6$ ), reaching calculated present day temperatures up to 166 °C in Greene County, Pennsylvania. The Mg—Li geothermometer calculated temperatures were similar to those calculated using the Na—Li geothermometer (generally within 10 % difference); however, Kharaka and Mariner (1989) indicate that there is a better correlation for oil field waters using the Mg—Li geothermometer. Caution is taken using geothermometers to estimate temperatures from gas wells which are likely lower than if measured in the field due to potential water vapor dilution of geochemical constituents (Kharaka and Mariner, 1989). Well production information was used to calculate GOR values and subsequently bin samples into hydrocarbon targets of dry gas, wet gas, and gas condensate that vary as a function of source rock thermal maturity (Table S1). GOR has been utilized as a proxy for source rock thermal maturity as GOR is itself a function of thermal maturity (Hickman et al., 2015; McDevitt et al., 2022; Zhang et al., 2017). More typically, thermal maturity of source rock is measured via vitrinite reflectance. The conodont alteration index (CAI) is an alternative thermal maturity measurement that is correlated with vitrinite reflectance but is completed less frequently due to the complexity of sample preparation (Hackley and Cardott, 2016; Repetski et al., 2006). A comprehensive study was previously completed using CAI for the Marcellus and Utica Shales and indicates a decreasing thermal maturity trend from the southeast to northwest, similar to the GOR value trend we report for produced water in this study (Repetski et al., 2008). UPP dry gas wells located at the largest depths, which correspond with the highest temperatures, are significantly associated with the lowest  $\delta^7\text{Li}$  values and highest Li concentrations (Fig. S5). This observation has important implications for simplified targeting of thermally mature dry gas wells in the UPP, and likely also applies in the more homogeneous dry gas hydrocarbon target of the overlying Marcellus Shale, for potential Li production.

While B and Li may be sourced from hydrocarbon-generating kerogen, previous studies have indicated that organic-associated Li is low compared to Li content in the recalcitrant silicate mineral fractions (i.e., clay minerals) of shales. Lithium is incorporated into clay minerals as an inner-layer cation substituting for Mg with increasing illitization of smectite (Jae Lee et al., 2024; Phan et al., 2016; Williams et al., 2013). The clay diagenesis of smectite to illite is closely associated with kerogen maturation, and both processes progress with increasing temperatures (Perry and Hower, 1970). Li concentration differences along a depth and temperature gradient within a given geologic unit, as reported here for the UPP, denote the importance for understanding the geologic heterogeneity (i.e., the variable source rock composition that impacts the geochemistry of formation brines) of a unit prior to targeting produced water for Li extraction.

A detailed depth and GOR analysis could not be completed for the other Appalachian Basin produced water samples (explicitly >90 days into production) due to a lack of published proprietary well information (i.e., API numbers). However, samples could be plotted by geologic age from youngest (Lower Mississippian) to oldest (Lower Ordovician) (Fig. 4). Because the Mg—Li geothermometer calculation inherently incorporates Li concentrations, Fig. 4 can be assessed solely for categorization purposes of geologic units represented. Notably, the shallowest Upper Devonian samples represent the lowest temperatures and smallest Li concentrations of the Appalachian Basin geologic units (Fig. 4). Deeper Appalachian Basin produced water Li concentrations from the Marcellus Shale, Lower Devonian (Oriskany Group), Lower Silurian (Clinton and Medina sandstones, Herkimer Limestone, and Oneida Conglomerate) and the UPP plot similarly for Li concentrations and calculated temperature (Fig. 4). Thus, higher reservoir temperatures, without considering fluid flow between the Middle Devonian and

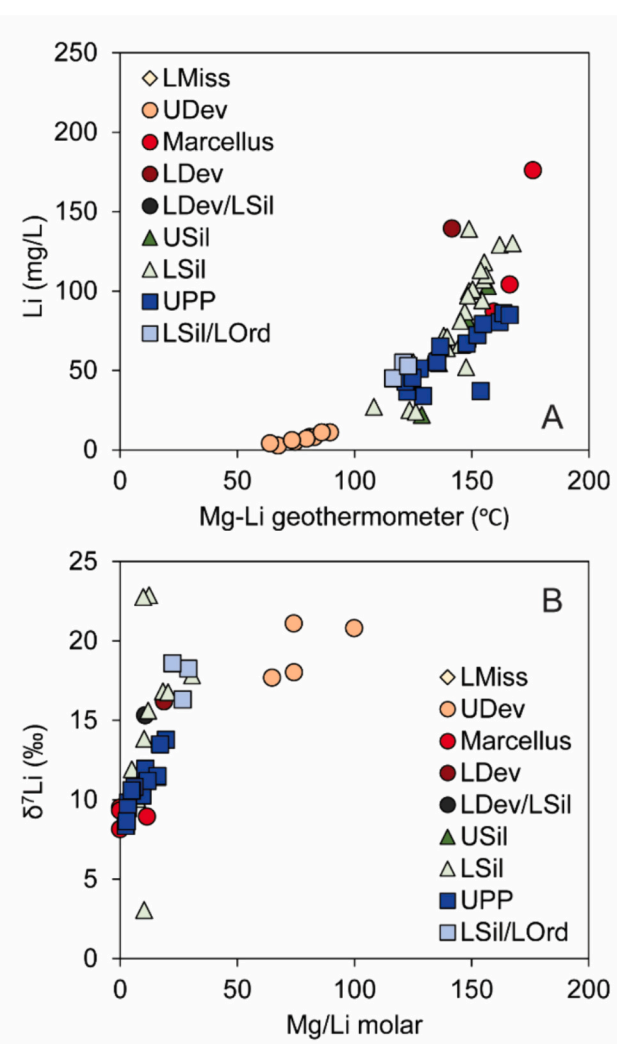


**Fig. 4.** A) Li concentrations as a function of the Mg—Li geothermometer and B)  $\delta^7\text{Li}$  as a function of the Mg/Li molar ratio for all available Appalachian Basin produced water samples collected from mature wells >90 days into production. Samples are plotted by geologic age in legend order of youngest to oldest. U and L stand for Upper and Lower, respectively. Miss, Dev, Sil, and Ord represent Mississippian, Devonian, Silurian, and Ordovician, respectively. UPP = Utica Shale and Point Pleasant Formation. Note that a few samples, namely the conventional road spreading samples collected from Pennsylvania townships, represent multiple geologic units and may geochemically reflect a fluid mixture.

Lower Ordovician, may serve as a reliable predictor for determining higher Li concentrations in Appalachian Basin produced water.

### 3.3. Produced water Mg/Li molar ratios indicate lower $\delta^7\text{Li}$ values and higher Li concentrations

Alkaline earth metal brine concentrations (Mg, Ca, Sr, Ba) are important considerations for controlling Li concentrations in produced water. Previous studies have indicated a link between Mg and Li concentrations because of association with clay mineral maturation at higher temperatures (Kharaka and Mariner, 1989; Vigier et al., 2008; Williams et al., 2013). Additionally, high fluid Mg concentrations at shallower UPP depths may stabilize smectite clay minerals and impede the illitization process, decreasing  $^6\text{Li}$  incorporation into the initial clay mineral structure (Mills et al., 2023). To avoid spurious correlations common in compositional data, major and trace element geochemistry of UPP samples (Blondes et al., 2020; Tasker et al., 2020) are plotted using a covariance centered log-ratio (clr)-biplot (Fig. S6). Additional

explanation of the method and interpretation is included in the Supporting Information. From this analysis, it is apparent that depth, Li concentration, and  $\delta^7\text{Li}$  values all vary systematically along the link that describes the bulk of geochemical variance, which is dominantly represented by the Mg/Li and Sr/Ca ratios. For the UPP, Li concentration is highest where (i) the Mg/Li ratios are lowest and Sr/Ca ratios are the highest, (ii) at the greatest depths, and (iii) where  $\delta^7\text{Li}$  values are the lowest (Fig. S6, Fig. S5). The Mg/Li molar ratio decreases significantly with UPP depth (Fig. S7,  $R^2 = 0.91, p = 1.2\text{E-}7$ ) while the Sr/Ca molar ratio increases significantly with UPP depth (Fig. S7,  $R^2 = 0.86, p = 1.7\text{E-}6$ ). The Mg/Li molar ratio is an important limiting factor for the chemical Li extraction process from brines because of the similarity in small radii and low molecular weight between the two elements. Because Li separation from brine with Mg/Li molar ratios  $>6$  can require pre-treatment to remove Mg (Zhao et al., 2013), the decrease of Mg/Li with increasing depth of the UPP brines infers favorable chemical conditions for Li extraction in the Li-rich deep UPP produced waters.

### 3.4. UPP core geochemistry and implications for temperature dependent fractionation modeling

The UPP Herrick 3H well core was analyzed for bulk rock geochemistry and  $\delta^7\text{Li}$  at 3 distinct depths (Table S2). The Herrick 3H well is located in Monroe County, Ohio, USA (Fig. 1). Generally, the Herrick 3H core is described as fine-grained shale that is interbedded with calcareous shale and silty mudstones that are organic-rich and fossiliferous (Brown et al., 2018). Minor calcite cement is also present. The highest Li bulk rock concentration measured was 80 mg/kg at the shallowest depth analyzed (3230.8 m) associated also with the highest Fe concentration, K concentration and Mg/Ca ratio. This Li concentration is similar to Marcellus Shale Li concentrations, previously reported to be upwards of 85 mg/kg (Phan et al., 2016). This UPP core depth of 3230.8 m also corresponded with the lowest percent loss on ignition (% LOI), indicating decreased presence of organic matter at this depth. Interestingly, this sample did not contain the lowest  $\delta^7\text{Li}$  value; the lowest value ( $-4.92\text{ \textperthousand} \pm 0.79\text{ \textperthousand}$ ) occurred at the intermediate core depth, which was also associated with the highest Mg/Li molar ratio (145) suggesting a temperature dependent fractionation of Li during illitization. The  $\delta^7\text{Li}$  value of  $-4.92\text{ \textperthousand}$  is important because this is the lowest  $\delta^7\text{Li}$  value measured in a shale sample to date. Phan et al. (2016) reported a Marcellus Shale core  $\delta^7\text{Li}$  value of  $-2.3\text{ \textperthousand} \pm 0.3\text{ \textperthousand}$  and Macpherson et al. (2014) summarized 13 global shale samples that had a mean  $\delta^7\text{Li}$  value of  $-0.2\text{ \textperthousand}$  and a median of  $-0.7\text{ \textperthousand}$ . Further, this measurement corroborates previous work by Macpherson et al. (2014) that sought to explain Marcellus and Upper Devonian aged produced water  $\delta^7\text{Li}$  measurements according to temperature dependent fractionation. The data they collected would have required a solid phase shale  $\delta^7\text{Li}$  value of approximately  $-5\text{ \textperthousand}$ . However, fluid in isotopic equilibrium with shale demonstrating an average measured core  $\delta^7\text{Li}$  of  $-0.4\text{ \textperthousand}$  best explains the UPP produced water  $\delta^7\text{Li}$  value assuming temperature-dependent fractionation ( $\delta^7\text{Li}_{\text{soln.}} = 7847/\text{T-}8.093 + \delta^7\text{Li}_{\text{shale}}$ , where T is in Kelvin (Millot et al., 2010a), Fig. 5). The observed geochemical variation across 80 m of UPP core provides important considerations for Li development in the Appalachian Basin, and other sedimentary basins, reflecting considerable heterogeneity in Li-host mineralogy, bulk rock geochemistry, and structural geologic features that may have impacted Li-host mineralogical alteration.

### 3.5. Li development potential in the Appalachian Basin compared to other U.S. geologic basins

While a Li resource estimate in the UPP is not the goal of this study, the applications of the Li source and enrichment mechanisms derived from isotopic compositions measured in this study have utility in decisions that impact Li development potential in the Appalachian Basin (e.g., geochemical heterogeneity within and between geologic units).

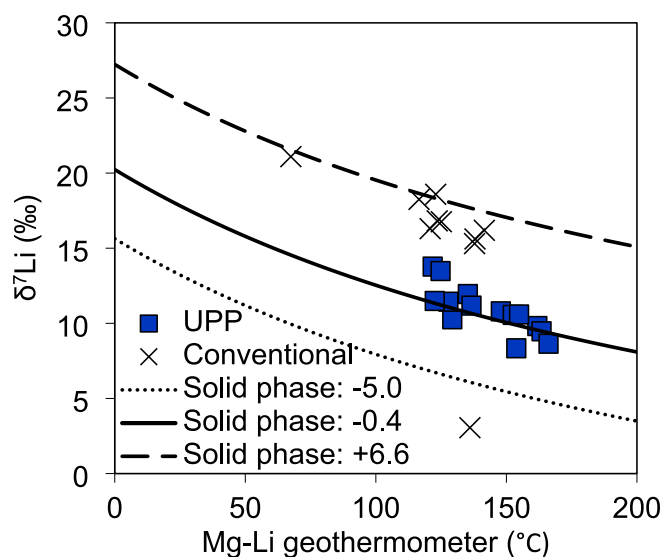


**Fig. 5.**  $\delta^7\text{Li}$  value versus calculated temperature for the Utica Shale and Point Pleasant Formation (UPP) and conventional produced water samples evaluated in this study. Trend lines represent produced water in isotopic equilibrium with a shale with a  $\delta^7\text{Li}$  value of  $-5.0\text{ \textperthousand}$  (approximately the lowest UPP core  $\delta^7\text{Li}$  measured),  $-0.4\text{ \textperthousand}$  (the average of the 3 UPP core  $\delta^7\text{Li}$  values measured), and  $+6.6\text{ \textperthousand}$  (the highest UPP core  $\delta^7\text{Li}$  value measured). The majority of  $\delta^7\text{Li}$  values of the UPP produced waters represent isotopic equilibrium with shale having a  $\delta^7\text{Li}$  value of  $-0.4\text{ \textperthousand}$ .

UPP samples from this study that were available in the S&P Global Commodity Insights (S&P Global Commodity Insights, 2023) database ( $n = 10$  of 14) have cumulative water production data available for each well lifetime. These volumes (L) were multiplied by the discrete produced water Li concentration (i.e., we assumed a constant lithium concentration in the produced water across the lifetime of the well) and converted to a total Li mass produced per well (kg). Over the six years in production, UPP 20 (located in Potter County, PA) generated produced water containing 1200 kg of Li in the form of wastewater, that, if it had been recovered, could have produced 6.4 metric tons of  $\text{Li}_2\text{CO}_3$  equivalent.

Well information was further mined from S&P Global Commodity Insights (S&P Global Commodity Insights, 2023) to compare the average estimated Li production between the Marcellus Shale and UPP. Formation producing names were searched in the database as “Utica Shale” and “Marcellus Shale” and yielded 244 and 14,417 wells, respectively. For the UPP, average cumulative water production was approximately 12.4 million L for an average well lifetime of 6.6 years yielding an average water production of approximately 2 million L/year/well. Multiplied by the average Li concentration in UPP produced water of 56 mg/L, UPP wells roughly produce an estimated 0.6 metric tons  $\text{Li}_2\text{CO}_3$  equivalent/year. For the Marcellus Shale, average cumulative water production was 7.2 million L for an average well lifetime of 8 years yielding an average water production of approximately 900,000 L/year/well. Multiplying this by the Marcellus produced water average Li concentration of 101 mg/L, Marcellus wells produce an estimated 0.5 metric tons of  $\text{Li}_2\text{CO}_3$  equivalent/year. Previous studies have reported Li mass recovery estimates for the Appalachian Basin in the highly permeable conventional Oriskany and Medina Groups (Dugamin et al., 2021) and the unconventional Marcellus Shale (Mackey et al., 2024), but no studies have yet compared Li mass estimates between the unconventional Marcellus and Utica Shales. Produced water volumetric studies are warranted to assess Li production on higher resolution temporal and spatial scale, including an assessment of Li mass production that may increase temporally throughout the well production lifetime.

Li demand, Li prices, and Li extraction technologies' development and economic viability can evolve rapidly. Li concentrations deemed economic also evolve rapidly with new extraction technologies making a specific Li concentration range difficult to pinpoint. Pilot scale Li extraction from formation brines with Li concentrations  $>100$  mg/L is currently occurring in the Smackover Formation in the Arkla/Louisiana-Mississippi Salt Basin of southern Arkansas. Standard Lithium Ltd. both processes the Li from waste bromine-extraction brines from LANXESS Corp. as LiCl<sub>2</sub> which is then processed into Li<sub>2</sub>CO<sub>3</sub> as well as directly extracts Li from the brines using a proprietary sorbent material (Standard Lithium, 2023). Additional studies assessing the potential for direct lithium extraction from other U.S.-sourced oil and gas produced waters are currently ongoing.

Appalachian Basin produced water samples have elevated Li concentrations when compared to other major oil and gas producing U.S. geologic basins (Fig. 6). Of the data available in the U.S. Geological Survey National Produced Water Geochemical Database (PWGD) (Blondes et al., 2018) that met the  $>90$  day sampling criteria ( $n = 6074$ ), only 279 individual produced water samples have Li concentrations  $>100$  mg/L (Fig. S8). Most of the samples with Li concentrations  $>100$  mg/L are located in the Appalachian, Arkla, Gulf Coast, and Williston Basins (Fig. S9) which agrees with data reported by other studies also utilizing the PWGD v2.3 (Marza et al., 2024). Arkla Basin produced water samples of the Smackover Formation have the highest reported Li concentrations upwards of 1700 mg/L, but were analyzed in the 1960s and represent statistical outliers compared to all other produced water Li values. Median Li concentrations are highest in Arkla (123.5 mg/L) followed by Appalachian (48.5 mg/L), Williston (28.3 mg/L) and Gulf Coast (7.6 mg/L) Basins (Fig. S9). Additionally, where available, Mg/Li molar ratios were also mapped with Li concentrations (Fig. 6). The highest Li concentrations in the PWGD are associated with low Mg/Li molar ratios ( $<1$ ) (Fig. 6) in agreement with previous studies indicating an association between high Li concentrations and low Mg/Li mass ratios (Dugamin et al., 2021). It is important to note that as a whole, U.S. produced water with the lowest Mg/Li molar ratios does not necessarily correlate to samples with the highest Li concentrations. There may be multiple explanations for this including important differences between hydrocarbon-hosted reservoir characteristics such as continuous versus conventional and the respective development differences between

reservoir type. Future studies could help to assess the differences between conventional and continuous hydrocarbon development and associated produced water Li content to further identify produced water for targeted Li extraction. As evidenced in the geochemical and geologic heterogeneity of the Appalachian Basin and UPP, specifically, presented throughout this study, elevated Li concentrations may exist within focused basin regions, emphasizing that basin specific Li source and enrichment mechanistic studies could inform targeted Li extraction.

#### 4. Conclusions

We present new  $\delta^7\text{Li}$ ,  $\delta^{11}\text{B}$ , and  $\delta^{138}\text{Ba}$  data for Appalachian Basin UPP produced water ( $n = 14$ ), conventional reservoir produced water ( $n = 10$ ), and UPP core samples from varied depths within the Herrick 3H well core ( $n = 3$ ). UPP produced water Li concentrations range from 33.7 to 85.9 mg/L while  $\delta^7\text{Li}$  ranged from  $8.34 \pm 0.90 \text{ ‰}$  to  $13.78 \pm 0.29 \text{ ‰}$ ,  $\delta^{11}\text{B}$  ranged from 26 to 35 ‰, and  $\delta^{138}\text{Ba}$  ranged from  $0.40 \pm 0.04 \text{ ‰}$  to  $2.49 \pm 0.03 \text{ ‰}$ , representing the highest  $\delta^{138}\text{Ba}$  value measured to date.  $\delta^7\text{Li}$  and  $\delta^{11}\text{B}$  values are significantly ( $p < 0.001$ ) higher in Appalachian Basin conventional produced water compared to unconventional Marcellus Shale and UPP produced water, while the  $\delta^{138}\text{Ba}$  value of conventional produced water is significantly lower than that of unconventional produced water ( $p < 0.005$ ). There are no significant differences between UPP and Marcellus Shale produced water  $\delta^7\text{Li}$ ,  $\delta^{11}\text{B}$ , or  $\delta^{138}\text{Ba}$  ( $p > 0.05$ ) values; however, Marcellus Shale produced water Li concentrations are significantly higher than that of UPP produced water.

Our new produced water isotopic data for the UPP suggest formation brine geochemical heterogeneity occurs along a depth and temperature-dependent hydrocarbon thermal maturity gradient. Li and B concentrations increase with UPP depth that is associated with increasing temperatures, increasing Sr/Ca molar ratios, decreasing Mg/Li molar ratios, and decreasing  $\delta^7\text{Li}$  and  $\delta^{11}\text{B}$  values. Together,  $\delta^7\text{Li}$ ,  $\delta^{11}\text{B}$ , and  $\delta^{138}\text{Ba}$  values likely indicate UPP Li sourcing from clay diagenesis and associated ion exchange during thermal maturation of the source rock. Additionally, we report the lowest  $\delta^7\text{Li}$  value measured in a shale sample to date ( $-4.92 \text{ ‰}$ ) corroborating previous studies invoking temperature dependent fractionation explanations of Li in the Marcellus Shale.

Appalachian Basin produced waters represent the second highest Li concentrations after the Arkla Basin. The highest Li concentrations for U.

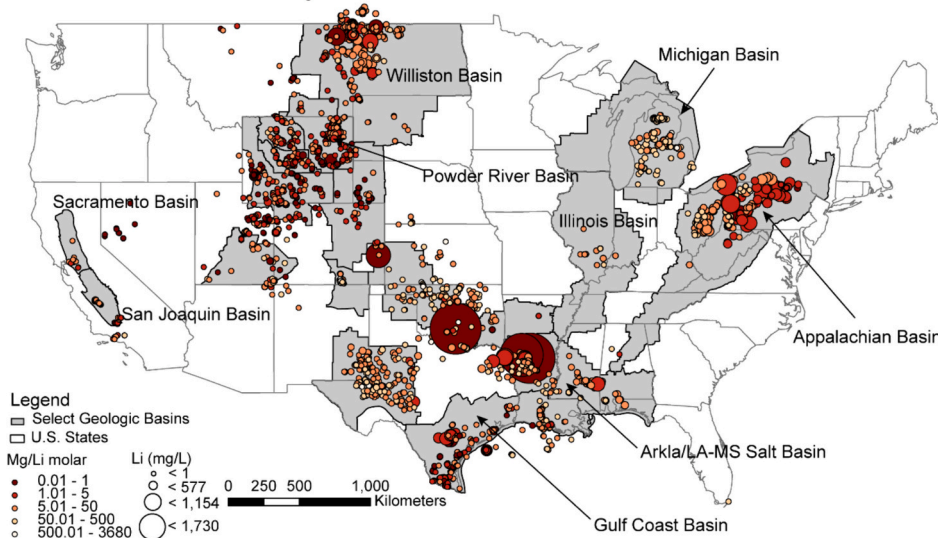


**Fig. 6.** Continental U.S. major oil and gas producing basins with available Li and Mg concentration data taken from the U.S. Geological Survey Produced Water Geochemical Database (Blondes et al., 2018) filtered for days  $>90$  when noted and removal of Li and Mg non-detects ( $n = 5308$ ). While the Arkla/LA-MS Salt Basin produced water Li concentrations are the highest reported, with two elevated datapoints measured in the 1960s, Appalachian Basin produced water Li concentrations are also frequently elevated compared to other geologic basin produced water. Note that highest Li concentrations occur where Mg/Li molar ratios are lowest ( $<1$ ) but the alternative is not necessarily true (i.e., many low Mg/Li molar ratios do not overlap with high Li concentrations).

S. produced water are associated with the lowest Mg/Li molar ratios. Knowledge gaps that impact Li extraction potential and resource estimates remain related to the heterogeneity of Li concentrations across U. S. sedimentary basins that include key hydrocarbon development differences between continuous and conventional reservoirs, brine production variability, temporal Li concentration differences during hydrocarbon production, and the basin-specific sources of and mechanisms for Li enrichment.

#### CRediT authorship contribution statement

**Bonnie McDevitt:** Writing – review & editing, Writing – original draft, Visualization, Project administration, Methodology, Investigation, Formal analysis, Data curation, Conceptualization. **Travis L. Tasker:** Writing – review & editing, Formal analysis, Data curation. **Rachel Coyte:** Writing – review & editing, Formal analysis, Data curation. **Madalyn S. Blondes:** Writing – review & editing, Writing – original draft, Formal analysis. **Brian W. Stewart:** Writing – review & editing, Writing – original draft, Formal analysis. **Rosemary C. Capo:** Writing – review & editing, Writing – original draft, Formal analysis. **J. Alexandra Hakala:** Writing – review & editing, Resources. **Avner Vengosh:** Writing – review & editing. **William D. Burgos:** Writing – review & editing. **Nathaniel R. Warner:** Writing – review & editing, Methodology, Investigation, Funding acquisition, Conceptualization.

#### Declaration of competing interest

The authors declare that they have no known competing financial interests or personal relationships that could have appeared to influence the work reported in this paper.

#### Data availability

Data are available in the Supplemental Information and as a U.S. Geological Survey data release: <https://doi.org/10.5066/P97N35DG>

#### Acknowledgements

The authors would like to thank Matthew Gonzales and Sara Kimmig from Penn State's LIME Lab for assistance with Li isotope method development. The authors would also thank Dustin Crandall from NETL for help acquiring Herrick 3H core samples. Oil and gas operators, as well as township supervisors, are thanked greatly for their cooperation in this study. This study was funded by U.S. Geological Survey Energy Resources Program (BM, MSB) and NSF Award number 1942601 for student support (TT). This study was also partially supported (RCC, BWS) by the U.S. Department of Energy's (DOE) Office of Fossil Energy as part of the National Energy Technology Laboratory's (NETL) ongoing research, and partly by appointments to the NETL research Participation Program, sponsored by the U.S. DOE and managed by the Oak Ridge Institute for Science and Education (ORISE). This project was funded by the U.S. Department of Energy, National Energy Technology Laboratory, in part, through a site support contract. Neither the U.S. Department of Energy nor any agency thereof, nor any of their employees, nor the support contractor, nor any of their employees, makes any warranty, express or implied, or assumes any legal liability or responsibility for the accuracy, completeness, or usefulness of any information, apparatus, product, or process disclosed, or represents that its use would not infringe privately owned rights. Reference herein to any specific commercial product, process, or service by trade name, trademark, manufacturer, or otherwise does not necessarily constitute or imply its endorsement, recommendation, or favoring by the U.S. Department of Energy or any agency thereof. The views and opinions of authors expressed herein do not necessarily state or reflect those of the U.S. Department of Energy or any agency thereof. Any use of trade, firm, or product names is for descriptive purposes only and does not imply

endorsement by the U.S. Government. Finally, the authors would like to thank Jenna Shelton and four anonymous reviewers for suggestions that greatly enhanced this manuscript.

#### Appendix A. Supplementary data

Supplementary data to this article can be found online at <https://doi.org/10.1016/j.scitotenv.2024.174588>.

#### References

Akob, D.M., Cozzarelli, I.M., Dunlap, D.S., Rowan, E.L., Lorah, M.M., 2015. Organic and inorganic composition and microbiology of produced waters from Pennsylvania shale gas wells. *Appl. Geochem.* 60 <https://doi.org/10.1016/j.apgeochem.2015.04.011>.

Akob, D.M., Mumford, A.C., Orem, W., Engle, M.A., Klinges, J.G., Kent, D.B., Cozzarelli, I.M., 2016. Wastewater disposal from unconventional oil and gas development degrades stream quality at a West Virginia injection facility. *Environ. Sci. Technol.* 50, 5517–5525. <https://doi.org/10.1021/acs.est.6b00428>.

Andrews, E., Pogge von Strandmann, P.A.E., Fantle, M.S., 2020. Exploring the importance of authigenic clay formation in the global Li cycle. *Geochim. Cosmochim. Acta* 289, 47–68. <https://doi.org/10.1016/j.gca.2020.08.018>.

Bates, S.L., Hendry, K.R., Pryer, H.V., Kinsley, C.W., Pyle, K.M., Woodward, E.M.S., Horner, T.J., 2017. Barium isotopes reveal role of ocean circulation on barium cycling in the Atlantic. *Geochim. Cosmochim. Acta* 204, 286–299. <https://doi.org/10.1016/j.gca.2017.01.043>.

Blondes, M.S., Gans, K.D., Engle, M.A., Kharaka, Y.K., Reidy, M.E., Saraswathula, V., Thordsen, J.J., Rowan, E.L., Morrissey, E.A., 2018. U.S. Geological Survey National Produced Waters Geochemical Database (ver. 2.3, January 2018) [WWW Document]. U.S. Geol. Surv. Data Release. <https://doi.org/10.5066/F7J964W8>.

Blondes, M.S., Shelton, J.L., Engle, M.A., Tremblay, J.P., Doolan, C.A., Jubb, A.M., Chenault, J.C., Rowan, E.L., Haefner, R.J., Mailot, B.E., 2020. Utica shale play oil and gas brines: geochemistry and factors influencing wastewater management. *Environ. Sci. Technol.* 54, 13917–13925. <https://doi.org/10.1021/acs.est.0c02461>.

Bridgestock, L., Nathan, J., Paver, R., Hsieh, Y.-T., Porcelli, D., Tanzil, J., Holdship, P., Carrasco, G., Vani, K.A., Swarzenski, P.W., Henderson, G.M., 2021. Estuarine processes modify the isotope composition of dissolved riverine barium fluxes to the ocean. *Chem. Geol.* 579, 120340 <https://doi.org/10.1016/j.chemgeo.2021.120340>.

Brown, S., Crandall, D., Moore, J., Mackey, P., Carr, T., Panetta, B., 2018. Computed Tomography Scanning and Geophysical Measurements of the Utica Shale from the Herrick 3H Well. National Energy Technology Laboratory. <https://doi.org/10.18141/143313.An>.

Bruner, K.R., Smosna, R., 2015. A Comparative Study of the Mississippian Barnett Shale, Fort Worth Basin, and Devonian Marcellus Shale, Appalachian Basin.

Burgos, W.D., Castillo-Meza, L., Tasker, T.L., Geeza, T.J., Drohan, P.J., Liu, X., Landis, J. D., Blotevogel, J., McLaughlin, M., Borch, T., Warner, N.R., 2017. Watershed-scale impacts from surface water disposal of oil and gas wastewater in Western Pennsylvania. *Environ. Sci. Technol.* 51, 8851–8860. <https://doi.org/10.1021/acs.est.7b01696>.

Cao, Z., Siebert, C., Hathorne, E.C., Dai, M., Frank, M., 2016. Constraining the oceanic barium cycle with stable barium isotopes. *Earth Planet. Sci. Lett.* 434, 1–9. <https://doi.org/10.1016/j.epsl.2015.11.017>.

Capo, R.C., Stewart, B.W., Rowan, E.L., Kolesar Kohl, C.A., Wall, A.J., Chapman, E.C., Hammack, R.W., Schroeder, K.T., 2014. The strontium isotopic evolution of Marcellus formation produced waters, southwestern Pennsylvania. *Int. J. Coal Geol.* 126, 57–63. <https://doi.org/10.1016/j.coal.2013.12.010>.

Chapman, E.C., Capo, R.C., Stewart, B.W., Kirby, C.S., Hammack, R.W., Schroeder, K.T., Edenborn, H.M., 2012. Geochemical and strontium isotope characterization of produced waters from marcellus shale natural gas extraction. *Environ. Sci. Technol.* 46, 3545–3553. <https://doi.org/10.1021/es204005g>.

Cozzarelli, I.M., Kent, D.B., Briggs, M., Engle, M.A., Bentham, A., Skalak, K.J., Mumford, A.C., Jaeschke, J., Farag, A., Lane, J.W., Akob, D.M., 2021. Geochemical and geophysical indicators of oil and gas wastewater can trace potential exposure pathways following releases to surface waters. *Sci. Total Environ.* 755, 142909. <https://doi.org/10.1016/j.scitotenv.2020.142909>.

Darvari, R., Nicot, J.P., Scanlon, B.R., Kyle, J.R., Elliott, B.A., Uhlman, K., 2024. Controls on lithium content of oilfield waters in Texas and neighboring states (USA). *J. Geochem. Explor.* 257, 107363. <https://doi.org/10.1016/j.gexplo.2023.107363>.

Delano, J.W., Schirnick, C., Bock, B., Kidd, S.F., Heizler, M.T., Putman, G.W., De Long, S. E., Ohr, M., 1990. Petrology and geochemistry of Ordovician K-bentonites in New York State: constraints on the nature of a volcanic arc. *J. Geol.* 98, 157–170. <https://doi.org/10.1086/629391>.

Dresel, P., Rose, A., 2010. Chemistry and origin of oil and gas well brines in western Pennsylvania. In: *Pennsylvania Geol. Surv., 4th Ser. Open ... 48. doi:Open-File Report OFOG 1001.0*.

Drollette, B.D., Hoelzer, K., Warner, N.R., Darrah, T.H., Karatum, O., O'Connor, M.P., Nelson, R.K., Fernandez, L.A., Reddy, C.M., Vengosh, A., Jackson, R.B., Elsner, M., Plata, D.L., 2015. Elevated levels of diesel range organic compounds in groundwater near Marcellus gas operations are derived from surface activities. *Proc. Natl. Acad. Sci. U. S. A.* 112, 13184–13189. <https://doi.org/10.1073/pnas.1511474112>.

Dugamin, E.J.M., Richard, A., Cathelineau, M., Boiron, M.C., Despinois, F., Brisset, A., 2021. Groundwater in sedimentary basins as potential lithium resource : a global prospective study. *Sci. Rep.* 1–10 <https://doi.org/10.1038/s41598-021-99912-7>.

Dugamin, E.J.M., Cathelineau, M., Boiron, M.C., Richard, A., Despinois, F., 2023. Lithium enrichment processes in sedimentary formation waters. *Chem. Geol.* 635, 121626. <https://doi.org/10.1016/j.chemgeo.2023.121626>.

Engle, M.A., Rowan, E.L., 2014. Geochemical evolution of produced waters from hydraulic fracturing of the Marcellus shale, northern Appalachian Basin: a multivariate compositional data analysis approach. *Int. J. Coal Geol.* 126, 45–56. <https://doi.org/10.1016/j.coal.2013.11.010>.

Evans, M.A., Battles, D.A., 1999. Fluid inclusion and stable isotope analyses of veins from the central Appalachian Valley and ridge province: implications for regional synorogenic hydrologic structure and fluid migration. *Bull. Geol. Soc. Am.* 111, 1841–1860. <https://doi.org/10.1130/0016-7606>.

Farnan, J., Vanden Heuvel, J.P., Dorman, F.L., Warner, N.R., Burgos, W.D., 2023. Toxicity and chemical composition of commercial road palliatives versus oil and gas produced waters. *Environ. Pollut.* 334, 122184. <https://doi.org/10.1016/j.envpol.2023.122184>.

Federal Register: U.S. Geological Survey, 2022. 2022 final list of critical minerals. *Fed. Regist.* 87 (37), 10381–10382.

Foster, G.L., Pogge Von Strandmann, P.A.E., Rae, J.W.B., 2010. Boron and magnesium isotopic composition of seawater. *Geochem. Geophys. Geosyst.* 11, 1–10. <https://doi.org/10.1029/2010GC003201>.

Geeza, T.J., Gillikin, D.P., McDevitt, B., Van Sice, K., Warner, N.R., 2018. Accumulation of Marcellus formation oil and gas wastewater metals in freshwater mussel shells. *Environ. Sci. Technol.* 52, 10883–10892. <https://doi.org/10.1021/acs.est.8b02727>.

Gong, Y., Zeng, Z., Cheng, W., Lu, Y., Zhang, L., Yu, H., 2020. Barium isotopic fractionation during strong weathering of basalt in a tropical climate. *Environ. Int.* 143, 105896. <https://doi.org/10.1016/j.envint.2020.105896>.

Groundwater Protection Council, 2022. U.S. Produced Water Volumes and Management Practices in 2021.

Hackley, P.C., Cardott, B.J., 2016. Application of organic petrography in North American shale petroleum systems: a review. *Int. J. Coal Geol.* 163, 8–51. <https://doi.org/10.1016/j.coal.2016.06.010>.

Harkness, J.S., Dwyer, G.S., Warner, N.R., Parker, K.M., Mitch, W.A., Vengosh, A., 2015. Iodide, bromide, and ammonium in hydraulic fracturing and oil and gas wastewaters: environmental implications. *Environ. Sci. Technol.* 49, 1955–1963. <https://doi.org/10.1021/es504654n>.

Hickman, J., Eble, C., Riley, R.A., Erenpreiss, M., Carter, K.M., Harper, J.A., Dunst, B., Smith, L., Cooney, M.L., Soeder, D., Metzger, G., Moore, J., Hohn, M.E., Pool, S., Saucer, J., Patchen, D.G., 2015. A Geologic Play Book for Utica Shale Appalachian Basin Exploration.

Horner, T.J., Kinsley, C.W., Nielsen, S.G., 2015. Barium-isotopic fractionation in seawater mediated by barite cycling and oceanic circulation. *Earth Planet. Sci. Lett.* 430, 511–522. <https://doi.org/10.1016/j.epsl.2015.07.027>.

Hsieh, Y.-T., Henderson, G.M., 2017. Barium stable isotopes in the global ocean: tracer of Ba inputs and utilization. *Earth Planet. Sci. Lett.* 473, 269–278. <https://doi.org/10.1016/j.epsl.2017.06.024>.

Hund, K., La Porta, D., Fabregas, T.P., Laing, T., Dreshage, J., 2020. Minerals for Climate Action: The Mineral Intensity of the Clean Energy Transition. Washington, D.C.

Jae Lee, K., You, J., Gao, Y., Terlier, T., 2024. Release, transport, and accumulation of lithium in shale brines. *Fuel* 356, 129629. <https://doi.org/10.1016/j.fuel.2023.129629>.

Jochum, K.P., Nohl, U., Herwig, K., Lammel, E., Stoll, B., Hofmann, A.W., 2005. GeoReM: a new geochemical database for reference materials and isotopic standards. *Geostand. Geoanal. Res.* 29, 333–338. <https://doi.org/10.1111/j.1751-908x.2005.tb0904.x>.

Kalderon-Asael, B., Katchinoff, J.A.R., Planavsky, N.J., Hood, A.V.S., Dellingar, M., Belfroid, E.J., Jones, D.S., Hofmann, A., Ossa, F.O., Macdonald, F.A., Wang, C., Isson, T.T., Murphy, J.G., Higgins, J.A., West, A.J., Wallace, M.W., Asael, D., Pogge von Strandmann, P.A.E., 2021. A lithium-isotope perspective on the evolution of carbon and silicon cycles. *Nature* 595, 394–398. <https://doi.org/10.1038/s41586-021-03612-1>.

Kassotis, C.D., Iwanowicz, L.R., Akob, D.M., Cozzarelli, I.M., Mumford, A.C., Orem, W. H., Nagel, S.C., 2016. Endocrine disrupting activities of surface water associated with a West Virginia oil and gas industry wastewater disposal site. *Sci. Total Environ.* 557–558, 901–910. <https://doi.org/10.1016/j.scitotenv.2016.03.113>.

Kaunda, R.B., 2020. Potential environmental impacts of lithium mining. *J. Energy Nat. Resour. Law* 38, 237–244. <https://doi.org/10.1080/02646811.2020.1754596>.

Kesler, S.E., Gruber, P.W., Medina, P.A., Keoleian, G.A., Eversen, M.P., Wallington, T.J., 2012. Global lithium resources: relative importance of pegmatite, brine and other deposits. *Ore Geol. Rev.* 48, 55–69. <https://doi.org/10.1016/j.oregeorev.2012.05.006>.

Kharaka, Y.K., Mariner, R.H., 1989. Chemical geothermometers and their application to formation waters from sedimentary basins. In: *Thermal History of Sedimentary Basins*, pp. 99–117.

Kirschbaum, M.A., Schenk, C.J., Cook, T.A., Ryder, R.T., Charpentier, R.R., Klett, T.R., Gaswirth, S.B., Tennyson, M.E., Whidden, K.J., 2012. Assessment of undiscovered oil and gas resources of the Ordovician Utica shale of the Appalachian Basin Province, 2012. *U.S. Geol. Surv. Fact Sheet* 2012-3116, 1–6.

Kolesar Kohl, C.A., Capo, R.C., Stewart, B.W., Wall, A.J., Schroeder, K.T., Hammack, R. W., Guthrie, G.D., 2014. Strontium isotopes test long-term zonal isolation of injected and Marcellus formation water after hydraulic fracturing. *Environ. Sci. Technol.* 48, 9867–9873.

Kondash, A.J., Albright, E., Vengosh, A., 2017. Quantity of flowback and produced waters from unconventional oil and gas exploration. *Sci. Total Environ.* 574, 314–321. <https://doi.org/10.1016/j.scitotenv.2016.09.069>.

Kondash, A.J., Lauer, N.E., Vengosh, A., 2018. The intensification of the water footprint of hydraulic fracturing. *Sci. Adv.* 4 <https://doi.org/10.1126/sciadv.aar5982>.

Kumar, A., Fukuda, H., Hatton, T.A., Lienhard, J.H., 2019. Lithium recovery from oil and gas produced water: a need for a growing energy industry. *ACS Energy Lett.* 4, 1471–1474. <https://doi.org/10.1021/acsenergylett.9b00779>.

Lauer, N.E., Warner, N.R., Vengosh, A., 2018. Sources of radium accumulation in stream sediments near disposal sites in Pennsylvania: implications for disposal of conventional oil and gas wastewater. *Environ. Sci. Technol.* 52, 955–962. <https://doi.org/10.1021/acs.est.7b04952>.

Lin, Y., Merli, M., Censi, P., Redfern, S.A.T., Zhao, Y., Yin, Q.Z., Zheng, M., Yu, X., Zhang, Y., Knapp, W.J., Tipper, E.T., 2024. Experimental and theoretical constraints on lithium isotope fractionation during brine evaporation and halite precipitation. *Geochim. Cosmochim. Acta* 374, 250–263. <https://doi.org/10.1016/j.gca.2024.03.003>.

Mackey, J., Bain, D.J., Lackey, G., Gardiner, J., Gulliver, D., Kutchko, B., 2024. Estimates of lithium mass yields from produced water sourced from the Devonian - aged Marcellus shale. *Sci. Rep.* 1–9 <https://doi.org/10.1038/s41598-024-58887-x>.

Macpherson, G.L., 2015. Lithium in fluids from Paleozoic-aged reservoirs, Appalachian Plateau region, USA. *Appl. Geochem.* 60, 72–77. <https://doi.org/10.1016/j.apgeochem.2015.04.013>.

Macpherson, G.L., Capo, R.C., Stewart, B.W., Phan, T.T., Schroeder, K., Hammack, R.W., 2014. Temperature-dependent Li isotope ratios in Appalachian Plateau and Gulf Coast Sedimentary Basin saline water. *Geofluids* 14, 419–429. <https://doi.org/10.1111/gfl.12084>.

Marza, M., Ferguson, G., Thorson, J., Barton, I., Kim, J., Ma, L., McIntosh, J., 2024. Geological controls on lithium production from basinal brines across North America. *J. Geochem. Explor.* 257, 107383. <https://doi.org/10.1016/j.jexplo.2023.107383>.

Matecha, R.M., Capo, R.C., Stewart, B.W., Thompson, R.L., Hakala, J.A., 2021. A single column separation method for barium isotope analysis of geologic and hydrologic materials with complex matrices. *Geochem. Trans.* 22, 1–9. <https://doi.org/10.1186/s12932-021-00077-z>.

Matecha, R.M., Xiong, W., Heck, W.F., Stewart, B.W., Capo, R.C., Hakala, J.A., 2022. Experimental investigation of barium sources and fluid–rock interaction in unconventional Marcellus shale wells using Ba isotopes. *Energy Fuel.* <https://doi.org/10.1021/acs.energyfuels.2c00118>.

McDevitt, B., Cavazza, M., Beam, R., Cavazza, E., Burgos, W.D., Li, L., Warner, N.R., 2020a. Maximum removal efficiency of barium, strontium, radium, and sulfate with optimum AMD-Marcellus flowback mixing ratios for beneficial use in the northern Appalachian Basin. *Environ. Sci. Technol.* 54, 4829–4839. <https://doi.org/10.1021/acs.est.9b07072>.

McDevitt, B., McLaughlin, M.C., Vinson, D.S., Geeza, T.J., Blotevogel, J., Borch, T., Warner, N.R., 2020b. Isotopic and element ratios fingerprint salinization impact from beneficial use of oil and gas produced water in the Western U.S. *Sci. Total Environ.* 716 <https://doi.org/10.1016/j.scitotenv.2020.137006>.

McDevitt, B., Geeza, T.J., Gillikin, D.P., Warner, N.R., 2021. Freshwater mussel soft tissue incorporates strontium isotopic signatures of oil and gas produced water. *ACS ES&T Water* 1, 2046–2056. <https://doi.org/10.1021/acs.estwater.1c00135>.

McDevitt, B., Jubb, A.M., Varonka, M.S., Blondes, M.S., Engle, M.A., Gallegos, T.J., Shelton, J.L., 2022. Dissolved organic matter within oil and gas associated wastewaters from U.S. unconventional petroleum plays: comparisons and consequences for disposal and reuse. *Sci. Total Environ.* 838, 156331. <https://doi.org/10.1016/j.scitotenv.2022.156331>.

McDevitt, B., Tasker, T., Coyte, R., Blondes, M.S., Stewart, B.W., Capo, R.C., Hakala, J.A., Vengosh, A., Burgos, W.D., Warner, N.R., 2024. Utica Shale and Point Pleasant Formation Isotopic Compositions: U.S. Geological Survey Data Release. Reston, VA. <https://doi.org/10.5066/P97N35DG>.

McLaughlin, M.C., Borch, T., McDevitt, B., Warner, N.R., Blotevogel, J., 2020. Water quality assessment downstream of oil and gas produced water discharges intended for beneficial reuse in arid regions. *Sci. Total Environ.* 713, 136607. <https://doi.org/10.1016/j.scitotenv.2020.136607>.

Millot, R., Scaillet, B., Sanjuan, B., 2010a. Lithium isotopes in island arc geothermal systems: Guadeloupe, Martinique (French West Indies) and experimental approach. *Geochim. Cosmochim. Acta* 74, 1852–1871. <https://doi.org/10.1016/j.gca.2009.12.007>.

Millot, R., Vigier, N., Gaillardet, J., 2010b. Behaviour of lithium and its isotopes during weathering in the Mackenzie Basin, Canada. *Geochim. Cosmochim. Acta*. <https://doi.org/10.1016/j.gca.2010.04.025>.

Mills, M.M., Sanchez, A.C., Boisvert, L., Payne, C.B., Ho, T.A., Wang, Y., 2023. Understanding smectite to illite transformation at elevated (> 100 °C) temperature: effects of liquid/solid ratio, interlayer cation, solution chemistry and reaction time. *Chem. Geol.* 615, 121214. <https://doi.org/10.1016/j.chemgeo.2022.121214>.

Mumford, A.C., Malone, K.O., Akob, D.M., Nettemann, S., Proctor, A., Ditty, J., Ulsamer, L., Lookenbill, J., Cozzarelli, I.M., 2020. Shale gas development has limited effects on stream biology and geochemistry in a gradient-based, multiparameter study in Pennsylvania. *Proc. Natl. Acad. Sci. U. S. A.* 117, 3670–3677. <https://doi.org/10.1073/pnas.1911458117>.

Osborn, S.G., McIntosh, J.C., Hanor, J.S., Biddulph, D., 2012. Iodine-129, 87Sr/ 86Sr, and trace elemental geochemistry of northern Appalachian Basin brines: evidence for basinal-scale fluid migration and clay mineral diagenesis. *Am. J. Sci.* 312, 263–287. <https://doi.org/10.2475/03.2012.01>.

Parker, R.L., 1967. Data of Geochemistry: Composition of the Earth's Crust, Geological Survey Professional Paper 440-D.

Patnode, K.A., Hittle, E., Anderson, R.M., Zimmerman, L., Fulton, J.W., 2015. Effects of high salinity wastewater discharges on unionid mussels in the allegheny river, Pennsylvania. *J. Fish Wildl. Manage.* 6, 55–70. <https://doi.org/10.3996/052013-JFWM-033>.

Paukert Vankeuren, A.N., Hakala, J.A., Jarvis, K., Moore, J.E., 2017. Mineral reactions in shale gas reservoirs: barite scale formation from reusing produced water as hydraulic

fracturing fluid. *Environ. Sci. Technol.* 51, 9391–9402. <https://doi.org/10.1021/acs.est.7b01979>.

Perry, E., Hower, J., 1970. Burial diagenesis in Gulf Coast Pelitic sediments. *Clay Clay Miner.* 18, 165–177. <https://doi.org/10.1346/CCMN.1970.0180306>.

Phan, T.T., Capo, R.C., Stewart, B.W., Graney, J.R., Johnson, J.D., Sharma, S., Toro, J., 2015. Trace metal distribution and mobility in drill cuttings and produced waters from Marcellus shale gas extraction: uranium, arsenic, barium. *Appl. Geochem.* 60, 89–103. <https://doi.org/10.1016/j.apgeochem.2015.01.013>.

Phan, T.T., Capo, R.C., Stewart, B.W., Macpherson, G.L., Rowan, E.L., Hammack, R.W., 2016. Factors controlling Li concentration and isotopic composition in formation waters and host rocks of Marcellus Shale, Appalachian Basin. *Chem. Geol.* <https://doi.org/10.1016/j.chemgeo.2015.11.003>.

Piotrowski, P.K., Tasker, T.L., Geeza, T.J., McDevitt, B., Gillikin, D.P., Warner, N.R., Dorman, F.L., 2020. Forensic tracers of exposure to produced water in freshwater mussels: a preliminary assessment of Ba, Sr, and cyclic hydrocarbons. *Sci. Rep.* 10, 1–12. <https://doi.org/10.1038/s41598-020-72014-6>.

Pistiner, J.S., Henderson, G.M., 2003. Lithium-isotope fractionation during continental weathering processes. *Earth Planet. Sci. Lett.* 214, 327–339. [https://doi.org/10.1016/S0012-821X\(03\)00348-0](https://doi.org/10.1016/S0012-821X(03)00348-0).

Pogge von Strandmann, P.A.E., James, R.H., van Calsteren, P., Gislasen, S.R., Burton, K.W., 2008. Lithium, magnesium and uranium isotope behaviour in the estuarine environment of basaltic islands. *Earth Planet. Sci. Lett.* 274, 462–471. <https://doi.org/10.1016/j.epsl.2008.07.041>.

Pogge von Strandmann, P.A.E., Frings, P.J., Murphy, M.J., 2017. Lithium isotope behaviour during weathering in the Ganges Alluvial Plain. *Geochim. Cosmochim. Acta* 198, 17–31. <https://doi.org/10.1016/j.gca.2016.11.017>.

Renock, D., Landis, J.D., Sharma, M., 2016. Reductive weathering of black shale and release of barium during hydraulic fracturing. *Appl. Geochem.* 65, 73–86. <https://doi.org/10.1016/j.apgeochem.2015.11.001>.

Repetski, J.E., Ryder, R.T., Harper, J.A., Trippi, M.H., 2006. Thermal maturity patterns in the Ordovician and Devonian of Pennsylvania using conodont color alteration index (CAI) and vitrinite reflectance (%Ro). *Northeast. Geol. Environ. Sci.* 28, 266–294.

Repetski, J.E., Ryder, R.T., Weary, D.J., Harris, A.G., Trippi, M.H., 2008. Thermal maturity patterns (CAI and %Ro) in upper Ordovician and Devonian rocks of the Appalachian Basin: a major revision of USGS map I-917–E using new subsurface collections. *U.S. Geol. Surv. Sci. Investig. Map* 3006 (26 pp).

Rowan, E.L., 2006. Burial and Thermal History of the Central Appalachian Basin, Based on Three 2-D Models of Ohio, Pennsylvania, and West Virginia. *U.S. Geol. Surv. Open-File Rep.* 2006-1019 35.

Rowan, E.L., Engle, M.A., Kirby, C.S., Kraemer, T.F., 2011. Radium Content of Oil- and Gas-Field Produced Waters in the Northern Appalachian Basin (USA): Summary and Discussion of Data. *USGS Sci. Investig. Rep* (38 pp).

Rowan, Elisabeth L., Engle, M.A., Kraemer, T.F., Schroeder, K.T., Hammack, R.W., Dougherty, M.W., 2015. Geochemical and isotopic evolution of water produced from middle Devonian Marcellus shale gas wells, Appalachian basin, Pennsylvania. *Am. Assoc. Pet. Geol. Bull.* 99, 181–206. <https://doi.org/10.1306/07071413146>.

Rudnick, R.L., Tomascak, P.B., Njo, H.B., Gardner, L.R., 2004. Extreme lithium isotopic fractionation during continental weathering revealed in spherolites from South Carolina. *Chem. Geol.* 212, 45–57. <https://doi.org/10.1016/j.chemgeo.2004.08.008>.

Ryder, R.T., Burruss, R.C., Hatch, J.R., 1998. Black shale source rocks and oil generation in the Cambrian and Ordovician of the central Appalachian Basin, USA. *Am. Assoc. Pet. Geol. Bull.* 82, 412–441. <https://doi.org/10.1306/e4fd2d9d-1732-11d7-8645000102c1865d>.

Ryder, R.T., Crangle, R.D., Trippi, M.H., Swezey, C.S., Lentz, E.E., Rowan, E.L., Hope, R.S., 2009. Geologic Cross Section D-D' Through the Appalachian Basin from the Findlay Arch, Sandusky County, Ohio to the Valley and Ridge Province, Hardy County, West Virginia: U.S. Geological Survey Scientific Investigations Map 3067. Reston, Virginia.

S&P Global Commodity Insights, 2023. Enerdeq US well history and production: database available from S&P Global Commodity Insights [WWW Document]. 15 Inverness W. East, Englewood, CO 80112, U.S.A. URL <https://sgpglobal.com/commodityinsights> (accessed 1.30.23).

Scanlon, B.R., Ikonnikova, S., Yang, Q., Reedy, R.C., 2020a. Will water issues constrain oil and gas production in the United States? *Environ. Sci. Technol.* 54, 3510–3519. <https://doi.org/10.1021/acs.est.9b06390>.

Scanlon, B.R., Reedy, R.C., Xu, P., Engle, M., Nicot, J.P., Yoxtheimer, D., Yang, Q., Ikonnikova, S., 2020b. Can we beneficially reuse produced water from oil and gas extraction in the U.S.? *Sci. Total Environ.* 717, 137085 <https://doi.org/10.1016/j.scitotenv.2020.137085>.

Spivack, A.J., Palmer, M.R., Edmond, J.M., 1987. The sedimentary cycle of the boron isotopes. *Geochim. Cosmochim. Acta* 51, 1939–1949. [https://doi.org/10.1016/0016-7037\(87\)90183-9](https://doi.org/10.1016/0016-7037(87)90183-9).

Stallworth, A.M., Chase, E.H., McDevitt, B., Marak, K., Freedman, M.A., Wilson, R.T., Burgos, W.D., Warner, N.R., 2021. Efficacy of oil and gas produced water as a dust suppressant. *Sci. Total Environ.* 799, 149347 <https://doi.org/10.1016/j.scitotenv.2021.149347>.

Standard Lithium, 2023. Arkansas Smackover projects [WWW document]. URL <https://www.standardlithium.com/projects/arkansas-smackover>.

Stewart, B.W., Chapman, E.C., Capo, R.C., Johnson, J.D., Graney, J.R., Kirby, C.S., Schroeder, K.T., 2015. Origin of brines, salts and carbonate from shales of the Marcellus formation: evidence from geochemical and Sr isotope study of sequentially extracted fluids. *Appl. Geochem.* 60, 78–88. <https://doi.org/10.1016/j.apgeochem.2015.01.004>.

Tasker, T.L., Burgos, W.D., Piotrowski, P., Castillo-Meza, L., Blewett, T.A., Ganow, K.B., Stallworth, A., Delompré, P.L.M., Goss, G.G., Fowler, L.B., Vanden Heuvel, J.P., Dorman, F., Warner, N.R., 2018. Environmental and human health impacts of spreading oil and gas wastewater on roads. *Environ. Sci. Technol.* 52, 7081–7091. <https://doi.org/10.1021/acs.est.8b00716>.

Tasker, T.L., Warner, N.R., Burgos, W.D., 2020. Geochemical and isotope analysis of produced water from the Utica/Point Pleasant Shale, Appalachian Basin. *Environ Sci Process Impacts.* <https://doi.org/10.1039/d0em00066c>.

Tieman, Z.G., Stewart, B.W., Capo, R.C., Phan, T.T., Lopano, C.L., Hakala, J.A., 2020. Barium isotopes track the source of dissolved solids in produced water from the unconventional Marcellus shale gas play. *Environ. Sci. Technol.* 54, 4275–4285. <https://doi.org/10.1021/acs.est.0c00102>.

Tomascak, P.B., 2004. Developments in the understanding and application of lithium isotopes in the earth and planetary sciences. *Rev. Mineral. Geochem.* 55, 153–195. <https://doi.org/10.2138/gsrmg.55.1.153>.

U.S. Department of Energy, 2023. *Critical Materials Assessment*.

U.S. Energy Information Administration, 2017. *Utica Shale Play Geology Review. Washington, D.C.*

U.S. Geological Survey, 2022. Reference Material Information Sheet USGS SGR-1, SGR-1a, and SGR-1b. <https://doi.org/10.1038/063215a0>.

Van Sice, K., Cravotta, C.A., McDevitt, B., Tasker, T.L., Landis, J.D., Puhr, J., Warner, N.R., 2018. Radium attenuation and mobilization in stream sediments following oil and gas wastewater disposal in western Pennsylvania. *Appl. Geochem.* 98, 393–403. <https://doi.org/10.1016/j.apgeochem.2018.10.011>.

Vengosh, A., Chivas, A.R., Starinsky, A., Kolodny, Y., Baozhen, Z., Pengxi, Z., 1995. Chemical and boron isotope compositions of non-marine brines from the Qaidam Basin, Qinghai, China. *Chem. Geol.* 120, 135–154. [https://doi.org/10.1016/0009-2541\(94\)00118-R](https://doi.org/10.1016/0009-2541(94)00118-R).

Vigier, N., Decarreau, A., Millot, R., Carignan, J., Petit, S., France-Lanord, C., 2008. Quantifying Li isotope fractionation during smectite formation and implications for the Li cycle. *Geochim. Cosmochim. Acta.* <https://doi.org/10.1016/j.gca.2007.11.011>.

Von Allmen, K., Böttcher, M.E., Samankassou, E., Nägler, T.F., 2010. Barium isotope fractionation in the global barium cycle : first evidence from barium minerals and precipitation experiments. *Chem. Geol.* 277, 70–77. <https://doi.org/10.1016/j.chemgeo.2010.07.011>.

Wang, W., Wu, Z., Huang, F., 2021. Equilibrium barium isotope fractionation between minerals and aqueous solution from first-principles calculations. *Geochim. Cosmochim. Acta* 292, 64–77. <https://doi.org/10.1016/j.gca.2020.09.021>.

Warner, N.R., Christie, C.A., Jackson, R.B., Vengosh, A., 2013. Impacts of shale gas wastewater disposal on water quality in Western Pennsylvania. *Environ. Sci. Technol.* 47 <https://doi.org/10.1021/es402165b>.

Warner, N.R., Darrah, T.H., Jackson, R.B., Millot, R., Kloppmann, W., Vengosh, A., 2014. New tracers identify hydraulic fracturing fluids and accidental releases from oil and gas operations. *Environ. Sci. Technol.* 48, 12552–12560. <https://doi.org/10.1021/es5032135>.

Warner, N.R., Ajemigbitse, M.A., Pankratz, K., McDevitt, B., 2022. Naturally occurring radioactive material (NORM). In: Stoltz, J., Bain, D., Griffin, M. (Eds.), *Environmental Impacts from the Development of Unconventional Oil and Gas Reserves*. Cambridge University Press, pp. 214–245. <https://doi.org/10.1017/9781108774178.012>.

Welch, S., Sheets, J.M., Daly, R.A., Hanson, A., Sharma, S., Darrah, T., Olesik, J., Lutton, A., Mouser, P.J., Wrighton, K.C., Wilkins, M.J., Carr, T., Cole, D.R., 2021. Comparative geochemistry of flowback chemistry from the Utica/point pleasant and marcellus formations. *Chem. Geol.* 564, 120041 <https://doi.org/10.1016/j.chemgeo.2020.120041>.

Welch, S.A., Sheets, J.M., Saelans, E., Saltzman, M.R., Newby, S.M., Darrah, T.H., Lutton, A., Olesik, J.W., DeFranco, K.C., Heraty, L.J., Sturchio, N.C., Cole, D.R., 2022. Chemical and isotopic evolution of flowback fluids from the Utica gas shale play, Eastern Ohio USA. *Chem. Geol.* 614, 121186 <https://doi.org/10.1016/j.chemgeo.2022.121186>.

Williams, L.B., Hervig, R.L., 2005. Lithium and boron isotopes in illite-smectite: the importance of crystal size. *Geochim. Cosmochim. Acta* 69, 5705–5716. <https://doi.org/10.1016/j.gca.2005.08.005>.

Williams, L.B., Wieser, M.E., Fennell, J., Hutzcheon, I., Hervig, R.L., 2001. Application of boron isotopes to the understanding of fluid-rock interactions in a hydrothermally stimulated oil reservoir in the Alberta Basin, Canada. *Geofluids* 1, 229–240. <https://doi.org/10.1046/j.1468-8123.2001.00016.x>.

Williams, L.B., Środoń, J., Huff, W.D., Clauer, N., Hervig, R.L., 2013. Light element distributions (N, B, Li) in Baltic Basin bentonites record organic sources. *Geochim. Cosmochim. Acta* 120, 582–599. <https://doi.org/10.1016/j.gca.2013.07.004>.

Wilson, J.M., Vanbriesen, J.M., 2012. Oil and gas produced water management and surface Pennsylvania. *Environ. Pract.* 14, 288–301.

Zhang, T., Sun, X., Milliken, K.L., Ruppel, S.C., Enriquez, D., 2017. Empirical relationship between gas composition and thermal maturity in Eagle Ford Shale, south Texas. *Am. Assoc. Pet. Geol. Bull.* 101, 1277–1307. <https://doi.org/10.1306/09221615209>.

Zhao, Z., Si, X., Liu, X., He, L., Liang, X., 2013. Li extraction from high mg/li ratio brine with LiFePO<sub>4</sub>/FePO<sub>4</sub> as electrode materials. *Hydrometallurgy* 133, 75–83. <https://doi.org/10.1016/j.hydromet.2012.11.013>.